UNIVERSIDADE FEDERAL DE MINAS GERAIS

FACULDADE DE MEDICINA

MOLECULAR MEDICINE POSTGRADUATE PROGRAM

Mariana Costa Rossette

THE ANTICANCER PROPERTIES OF FLAVOKAWAIN B, A KAVA-KAVA COMPOUND, TOWARDS OVARIAN CANCER CELLS AND ITS ANTIANGIOGENIC ACTION *IN VIVO* AND *IN VITRO*

Belo Horizonte

2016

Mariana Costa Rossette

THE ANTICANCER PROPERTIES OF FLAVOKAWAIN B, A KAVA-KAVA COMPOUND, TOWARDS OVARIAN CANCER CELLS AND ITS ANTIANGIOGENIC ACTION *IN VIVO* AND *IN VITRO*

Doctoral thesis submitted to the Postgraduate program of Molecular Medicine at Universidade Federal de Minas Gerais, as a partial requirement for obtaining the title of PhD in Molecular Medicine.

Concentration area: *Molecular Medicine*

Supervisor: *Prof. Luiz Armando De Marco*

Belo Horizonte

2016

UNIVERSIDADE FEDERAL DE MINAS GERAIS

PROGRAMA DE PÓS-GRADUAÇÃO EM MEDICINA MOLECULAR

ATA DA DEFESA DE TESE DA ALUNA
MARIANA COSTA ROSSETTE

Realizou-se, no dia 03 de maio de 2016, às 09:00 horas, Fac Medicina, da Universidade Federal de Minas Gerais, a defesa de tese, intitulada *THE ANTICANCER PROPERTIES OF FLAVOKAWAIN B, A KAVA-KAVA COMPOUND, TOWARDS OVARIAN CANCER CELLS AND ITS ANTIANGÍOGENIC ACTION IN-VITRO AND IN-VIVO*, apresentada por MARIANA COSTA ROSSETTE, número de registro 2013707007, graduada no curso de MEDICINA, como requisito parcial para a obtenção do grau de Doutor em MEDICINA MOLECULAR, à seguinte Comissão Examinadora: Prof(a). Luiz Armando Cunha de Marco - Orientador (UFMG), Prof(a). Kenneth John Gollob (IEP - SANTA CASA), Prof(a). Antoniana Ursine Krettli (FIOCRUZ), Prof(a). Eitan Friedman (Tel Aviv University), Prof(a). Maria Jose Campagnole dos Santos (Universidade Federal de Minas Gerais).

A Comissão considerou a tese:

(X) Aprovada

( ) Reprovada

Finalizados os trabalhos, lavrei a presente ata que, lida e aprovada, vai assinada por mim e pelos membros da Comissão.
Belo Horizonte, 03 de maio de 2016.

Prof(a). Luiz Armando Cunha de Marco (Doutor)

Prof(a). Kenneth John Gollob (Doutor)

Prof(a). Antoniana Ursine Krettli (Doutora)

Prof(a). Eitan Friedman (Doutor)

Prof(a). Maria Jose Campagnole dos Santos (Doutora)

UNIVERSIDADE FEDERAL DE MINAS GERAIS

PROGRAMA DE PÓS-GRADUAÇÃO EM MEDICINA MOLECULAR

FOLHA DE APROVAÇÃO

THE ANTICANCER PROPERTIES OF FLAVOKAWAIN B, A KAVA-KAVA COMPOUND, TOWARDS OVARIAN CANCER CELLS AND ITS ANTIANGIOGENIC ACTION IN-VITRO AND IN-VIVO

MARIANA COSTA ROSSETTE

Tese submetida à Banca Examinadora designada pelo Colegiado do Programa de Pós-Graduação em MEDICINA MOLECULAR, como requisito para obtenção do grau de Doutor em MEDICINA MOLECULAR, área de concentração MEDICINA MOLECULAR.

Aprovada em 03 de maio de 2016, pela banca constituída pelos membros:

Prof(a). Luiz Armando Cunha de Marco - Orientador
UFMG

Prof(a). Kenneth John Gollob
IEP - SANTA CASA

Prof(a). Antoniana Ursine Krettli
FIOCRUZ

Prof(a). Eitan Friedman
Tel Aviv University

Prof(a). Maria Jose Campagnole dos Santos
Universidade Federal de Minas Gerais

Belo Horizonte, 3 de maio de 2016.

To my parents, sister, fiancé and dearest friends,

for their support, encouragement and unconditional love.

ACKNOWLEDGEMENTS

I wish to express my sincere gratitude to my advisor Professor Luiz Armando De Marco for the great opportunity to learn about science and to go beyond the books and guidelines seeking for new knowledge about this challenging disease, called cancer. Thank you for being an example of researcher, professor and human being.

I am very grateful to Dr. Hanna Caldas for giving me the opportunity to work and learn in her laboratory in 2009, where I started to study about Flavokawain B. Thank you for being so kind, teaching me valuable skills and encouraging me to continue this research.

I also sincerely thank Dr. Maria José Campagnole for teaching me about research for the first time, inspiring me to love it and for the great opportunity to go to Wake Forest University as an exchange student.

To Dr. Eitan Friedman and Dr. Luciana Bastos Rodrigues, I express my appreciation for being a constant source of motivation, helping me with new ideas and precious advice for this work.

I am extremely thankful and hugely indebted to Débora Chaves Moraes, my collaborator and close friend. I couldn't have done this project without you. Thank you for being present, incredibly hard-working and believing in this research as I do.

I would also like to thank Erika Kelmer, my collaborator, who has brilliantly made the zebrafish studies possible and performed all the angiogenesis studies together with us.

I also acknowledge Dr. Luiz Alexandre Magno, Dr. Daniela Valadão, Dr. Alexandre Barros, Dr. Luiza Martins, Dr. Karen Torres, Dr. Carolina Aguiar, Dr. Vitor Rezende, Dr. Juliana Carvalho and Dr. Dawidson Gomes for the support and advice during the experiments.

To all our current and past laboratory staff, I extend my deepest gratitude for the research suggestions, words of motivation and friendship, especially Flávia Melo, Helena Sarubi, Patrícia Couto, Cristina Sábato and Nayra Soares.

I want to express my gratitude to Dr. José Renan and all his laboratory staff for being so kind, receptive and allowing me to use their cell culture room, so I could finish my *in vitro* studies.

To the Coordenação de Aperfeiçoamento de Pessoal de Nível Superior (CAPES) for the scholarship in the CAPES-FIPSE and PhD programs.

To my parents, Elizabete and Altair, I'm eternally grateful for giving me the opportunity to follow my dreams and making them a reality.

I thank my sister, Raquel and nephew, Arthur for being a constant source of happiness.

Hálisson Flamini, my fiancé, your understanding, love and words of encouragement have made this possible.

To God for being my constant source of faith, strength and life.

“Learn from yesterday, live for today, hope for tomorrow. The important thing is not to stop questioning.”

Albert Einstein

ABSTRACT

Natural products have been utilized for centuries as novel compounds for the treatment and prevention of many diseases. The anticancer potential of chalcones in the Kava-kava extract, a plant grown in the Pacific Islands, have been inferred from the correlation with kava consumption and lower incidence of cancer in these populations. Flavokawain B, a naturally occurring chalcone of kava-kava, has shown impressive anti-cancer effects in several studies, besides other significant anti-inflammatory and antinociceptive activities. Epithelial ovarian cancer (EOC) is the most lethal gynecologic malignancy and the fifth most common cause of cancer-related deaths in woman. Current treatment with surgery and chemotherapy has improved survival; however recurrence and disease progression occurs in approximately 80% of patients in advanced stage. The development of more effective treatment strategies is urgent and many studies are being done in order to develop target chemotherapeutics against ovarian cancer molecular pathogenesis pathways, such as antiangiogenic drugs, PARP and PI3K inhibitors. In the present work we identified, for the first time, flavokawain B as causing strong antiproliferative and apoptotic effects against ovarian cancer cells with less cytocidal action against normal cells. Flavokawain B results in downregulation of Bcl-2 anti-apoptotic protein expression, increased Bax:Bcl-2 ratio and a significant dose-dependent inhibition of Akt activation on OVCAR-3 cells. These are important findings, since Bcl-2 overexpression and Akt overactivation are frequently associated with poor prognosis and resistance to chemotherapy in ovarian cancer. In addition, this work has demonstrated the strong antiangiogenic action of FKB *in vitro* and *in vivo* utilizing a zebrafish model. Altogether, we

believe that FKB might be a promising weapon in the arsenal of treatment options against ovarian cancer.

RESUMO

Produtos naturais têm sido utilizados por séculos no tratamento e prevenção de muitas doenças. O potencial anti-carcinogênico das chalconas obtidas do extrato da planta Kava-kava, comumente cultivada nas Ilhas do Pacífico, tem sido inferido a partir da correlação do consumo de kava e a baixa incidência de câncer nestas regiões. A Flavokawaína B (FKB), uma chalcona natural presente no extrato de kava, demonstrou efeitos anti-carcinogênicos, anti-inflamatórios e anti-nociceptivos significativos em diversos estudos. O câncer de ovário epitelial é a neoplasia ginecológica mais letal e quinta causa de morte relacionada ao câncer entre mulheres. O tratamento atual que consiste em cirurgia e quimioterapia melhorou a sobrevida, porém recidivas e progressão da doença ocorrem em aproximadamente 80% dos pacientes com doença avançada. O desenvolvimento de novas estratégias mais efetivas de tratamento é urgente e muitos estudos estão sendo realizados para o desenvolvimento de quimioterápicos que atuem sobre as vias moleculares patogênicas do câncer ovariano, como por exemplo as drogas anti-angiogênicas, inibidores da PARP e PI3K. No presente estudo identificamos, pela primeira vez, grande atividade anti-proliferativa e apoptótica da flavokawaína B contra células de câncer ovariano, além de menor efeito citotóxico da FKB contra células normais. A FKB resultou em redução da expressão da proteína anti-apoptótica Bcl-2, aumento da razão de Bax:Bcl-2 e inibição significativa e dose-dependente da ativação de Akt em células OVCAR-3. Considerando que a super-expressão de Bcl-2 e super-ativação de Akt estão relacionados ao pior prognóstico e resistência à quimioterapia no câncer de ovário, tais achados são importantes. Além disso, demonstramos que a FKB possui grande atividade anti-angiogênica *in vitro* e *in vivo*

utilizando um modelo de zebrafish. Esses resultados revelam que a FKB é um agente promissor no arsenal de opções terapêuticas contra o câncer de ovário.

LIST OF FIGURES

LIST OF TABLES

LIST OF ABREVIATIONS AND SYMBOLS

α	alpha
β	beta
µ	micro
µg	micrograms
µm	micrometer
µM	micromolar
143B	Human bone osteosarcoma cells
22RV1	Human prostate cancer cells
4-T1	Mouse mammary carcinoma
7- AAD	7-aminoactinomycin D
A-2058	Human melanoma cells
A549	Human lung adenocarcinoma
ACC-2	Adenoid cystic carcinoma
ADP	Adenosine diphosphate
AEBSF	4-(2-Aminoethyl) benzenesulfonyl fluoride hydrochloride
AIF	Apoptosis Inducing Factor
Akt	v-akt murine thymoma viral oncogene homolog 1
AP	Alkaline phosphatase
Apaf-1	Apoptotic protease activating factor 1
AR	Androgen receptor
Bad	B-cell lymphoma -associated death promoter
Bak	B-cell lymphoma 2 homologous antagonist/killer
Bax	B-cell lymphoma 2-associated X protein
BCIP	5-Bromo-4-chloro-3-indolyl phosphate disodium salt
Bcl-2	B-cell lymphoma 2
Bcl-xL	B-cell lymphoma-extra large
BCRJ	Banco de células do Rio de Janeiro
Bid	BH3 interacting-domain death agonist
Bik	B-cell lymphoma 2 -interacting killer
Bim	B-cell lymphoma 2 interacting mediator of Cell Death

BRAF	v-raf murine sarcoma viral oncogene homolog B1
BRCA1	Breast cancer 1, early onset
BRCA2	Breast cancer 2, early onset
C4-2B	Human prostate cancer cells
Ca Ski	Carcinoma of the cervix
$CaCl_2$	Calcium chloride
Cal-27	Oral squamous carcinoma cells
CO_2	Carbon dioxide
COX-I	Ciclo-oxigenase-1
COX-II	Ciclo-oxigenase-2
CXCR4	Chemokine receptor type 4
DAPI	4,6-diamidino-2-phenylindole
DMEM	Dulbecco's modified Eagle's medium
DMSO	Dimethyl sulfoxide
DNA	Deoxyribonucleic acid
DR5	Death receptor 5
DU145	Human prostate cancer cells
ECC-1	Human endometrial adenocarcinoma cells
EJ	Human bladder carcinoma
EOC	Epithelial ovarian cancer
ERBB2	Erb-B2 Receptor Tyrosine Kinase 2
FBS	Fetal bovine serum
FDA	Food and Drug Administration
FK	Flavokawain
FKA	Flavokawain A
FKB	Flavokawain B
FKC	Flavokawain C
h	hour
H460	Human lung large cell carcinoma
HBMEC	Human brain microvascular endothelial cells
HCT 116	Human colon carcinoma
HepG2	Hepatoma cells
HFW	Human fibroblast cells

HGF	Human gengival fibroblast cells
HGSOC	High grade serous ovarian cancer
HSC-3	Human oral carcinoma cells
HS-SY-II	Humal synovial sarcoma cells
HUVEC	Human umbilical vein endothelial cells
IC_{50}	Maximal inhibitory concentration
INCA	Instituto Nacional de Câncer
iNOS	Inducible nitric oxide synthase
IP	Intraperitoneal
IV	Intravenous
KB	Oral epidermal carcinoma
KCl	Potassium Chloride
kDa	Kilodaltons
KH_2PO_4	Potassium Dihydrogen Phosphate
KRAS	Kirsten rat sarcoma viral oncogene homolog
L-02	Normal immortalized liver cells
LANCaP	Human prostate cancer cells
LAPC4	Human prostate cancer cells
LPS	Lipopolysaccharide
LVES	Large Vessel Endothelial Supplement
M	Molar
MAPK	Mitogen-activated protein kinases
MCF-7	Human breast adenocarcinoma cell line
MDA-MB231	Human breast adenocarcinoma cell line
MG-63	Human bone osteosarcoma cells
$MgCl_2$	Magnesium chloride
$MgSO_4$	Magnesium sulfate
min	Minutes
mL	Milliliters
MMP-9	Matrix-metalloproteinase 9
mRNA	Messenger ribonucleic acid
mTOR	Mammalian Target of Rapamycin
MTT	3-(4,5-dimethylthiazol-2-yl)-2,5-diphenyltetrazolium bromide

Na_2PO_4	Disodium Phosphate
NaCl	Sodium Chloride
$NaHCO_3$	Sodium bicarbonate
NBT	Nitroblue tetrazolium
NBT	Nitro-blue tetrazolium
NF1	Neurofibromatosis type 1 gene
NF-kB	Nuclear factor kappa B
NIH3T3	Human fibroblast cells
NTMT	Alkaline phosphatase buffer
OC	Ovarian cancer
OS160	Human bone osteosarcoma cells
OVCAR-3	Ovarian cancer adenocarcinoma cells
PARP	Poly (adenosine diphosphate-ribose) polymerase
PBS	Phosphate Buffer Saline
PBT	Phosphate buffered saline with 0.1% tween 20
PC-3	Human prostate cancer cells
PDK1	Pyruvate dehydrogenase lipoamide kinase isozyme 1
hpf	Hours post fertilization
PFS	Progression free survival
PI	Propidium Iodide
PI3K	Phosphatidylinositide 3-kinase
PIK3CA	Phosphatidylinositol-4,5-Bisphosphate 3-Kinase, Catalytic Subunit Alpha
PIP_2	Phosphatidylinositol 4,5-bisphosphate
PIP_3	Phosphatidylinositol (3,4,5)-trisphosphate
PIP_3	Phosphatidylinositol-4,5-bisphosphate 3-kinase
PrECs	Human prostate epithelial cells
PrECs	Human prostate stromal cells
PTEN	Phosphatase and tensin homolog
Puma	p53 upregulated modulator of apoptosis
RAW 264.7	Murine macrophage cells
RPMI	Roswell Park Memorial Institute
RT4	Human urinary bladder transitional papilloma cell line
Saos-2	Human bone osteosarcoma cells

SDF-1	Stromal cell-derived factor 1
SDS	Sodium dodecyl sulfate
Ser473	Serine 473
SIV	Subintestinal vein
SK-LMS-1	Human uterine leiomyosarcoma cells
STIC	Serous tubal intraepithelial carcinomas
SYO	Human synovial sarcoma cells
SNAIL	Zinc finger protein
T24	Human urinary bladder transitional carcinoma cell line
T75	75 cm^2 tissue culture flask
T-HESC	Human endometrium fibroblast cells
Thr308	Threonine 308
TI	Therapeutic index
Tie-2	Receptor tyrosine kinase of angiopoietin
TNF-α	Tumor necrosis factor alpha
TP53	Tumor protein p53
TSP-2	Thrombospondin 2
u-PA	Urokinase plasminogen activator
USA	United the States of America
VEGF	Vascular endothelial growth factor
XIAP	X-linked inhibitor of apoptosis protein

SUMMARY

1 INTRODUCTION

1.1 Kava-Kava

1.1.1 Kava-kava plant and beverage

Kava-kava plant, *Piper methysticum* or intoxicating pepper is a robust, perennial shrub belonging to the *Piperaceae* family. It grows in stony ground, reaching heights from 4 to 6 meters. The leaves are green, heart-shaped, pointed and have about 15 cm in length. The roots grow about 60 cm bellow the ground and can become considerably thick at maturity (Figure 1) (Singh, 1992).

Figure 1: An adult Piper methysticum plant, named popularly Kava-Kava. Leaves (A) and Roots (B) Images available at <www.wikipedia.com>, accessed on October 01, 2015.

Kava plant can be found in various parts of the world, but is most commonly encountered in nearly all the Pacific islands. Its beverage is traditionally used for social and religious purposes. with the exceptions of New Zealand, New Caledonia and most of the Soloman Islands. Figure 2 shows the geographical locations of most of the kava-drinking

regions in Oceania, which is encompassed by the three cultural and ethnic regions of Melanesia, Polynesia and Micronesia (Singh, 1992; Steiner, 2000).

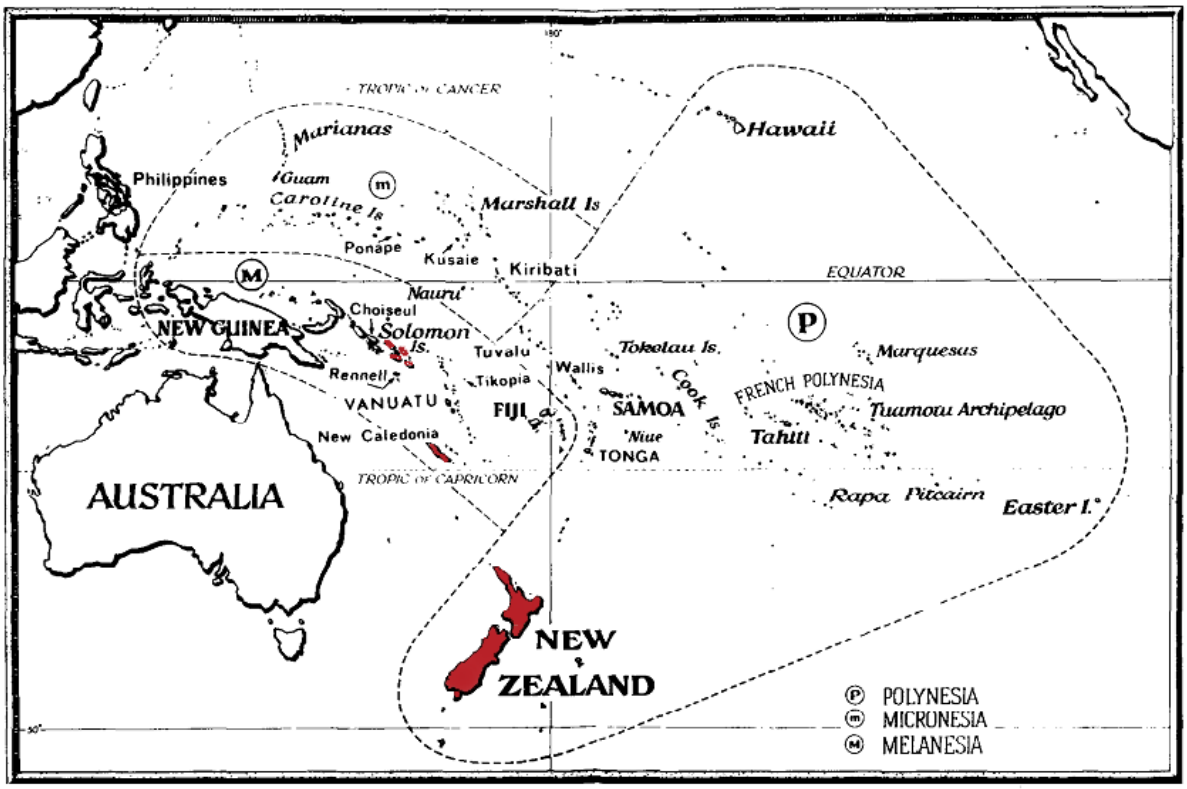

Figure 2: South Pacific islands. Map of Oceania showing most of the Kava drinking countries and the three cultural regions of Melanesia, Micronesia and Polynesia. Non-kava drinking countries are represented in red. (Reproduced from Singh, 1992)

For kava beverage preparation, roots are ground and mixed with water or coconut water and the drink is traditionally used mainly for men during a ceremony (Figure 3). After drinking, kava is found to reduce fatigue, anxiety and to produce pleasant, cheerful and sociable attitude (Steiner, 2000; Sharver, 2014).

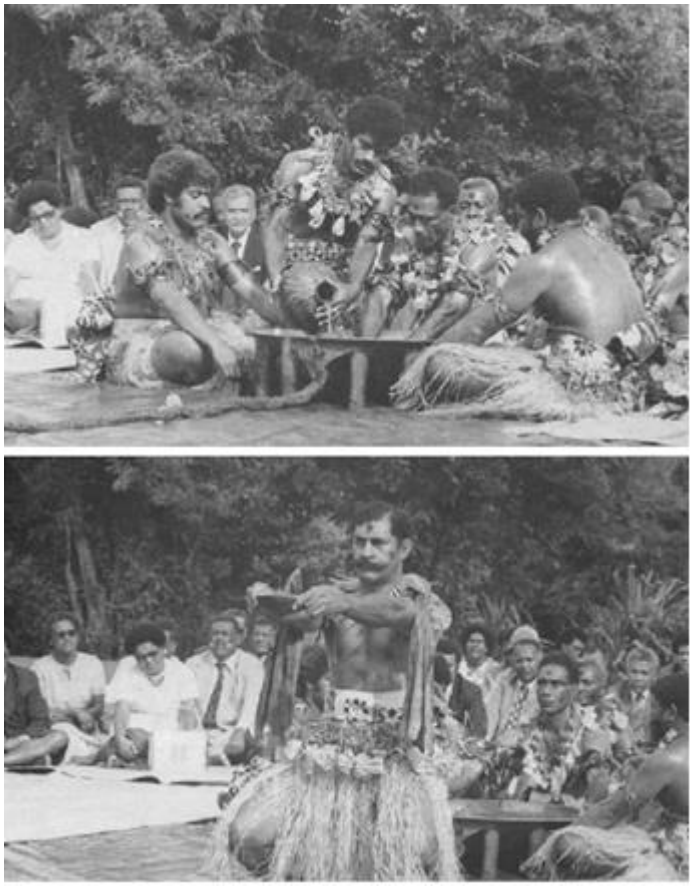

Figure 3 : Kava ceremony in Fiji. Kava is prepared in a utensil called *tanoa* where water is poured and mixed with kava roots. Only men are permitted to officiate the ceremony.
(Reproduced from Singh YN. Kava: an overview. *Journal of Ethnopharmacol* 1992).

The use of Kava in medicinal practices has been dated back to the eighteenth century for many purposes -anti-anxiety, antidepressant, muscle relaxant, analgesic, anti-convulsant, in the treatment of chronic cystitis, asthma, syphilis and gonorrhea (Singh, 1992; Steiner, 2000). In the past 20 years, organic solvent extracts from kava roots have also been used in Western countries, leading to its emergence as one of the 10 best-selling botanical supplements for the treatment of anxiety and depression (Zhou *et al.*, 2010). Despite the safety of traditional kava drinking in South Pacific Islands, severe side effects of liver damage were reported in Europe and United the States of America (USA) after the use of commercial preparations (Zhou *et al.*, 2010; Teschke *et al*., 2011).

1.1.2 Chemical properties

There are 2 major classes of compounds found within the Kava roots extract: kavalactones and chalcones. Kavalactones, the major components of kava and responsible for psychoactive effects, include: kawain, methysticin, desmethoxyyangonin and yangonin. The chalcones are Flavokawain A (FKA), Flavokawain B (FKB), and Flavokawain C (FKC), representing 0.46%, 0.015% and 0.012% of kava root extracts respectively. These compounds have similar backbones with different side chains (Singh, 1992; Zi & Simoneau, 2005). FKA contains a methoxy group, FKB only hydrogen and FKC has an extra hydroxyl group (Table 1) (Singh, 1992; Zi & Simoneau, 2005; Abu *et al.*, 2013).

Table 1: Summary of the molecular properties of Kava-kava chalcones.

Properties	Flavokawain A	Flavokawain B	Flavokawain C
Molecular weight	314.33g/mol	284.31g/mol	300.31g/mol
Molecular formula	$C_{18}H_{18}O_5$	$C_{17}H_{16}O_4$	$C_{17}H_{16}O_5$
Molecular structure	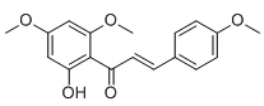	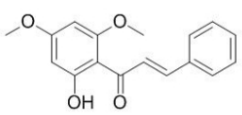	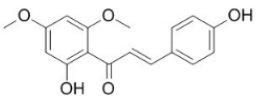

Modified from Abu *et al.*, 2013. Images in the table are available at < http://www.albtechnology.com>, accessed on January 10, 2016.

Chalcones are precursor of flavonoids in plants, which have shown to have many biological activities including antioxidant, anti-inflammatory and anti-cancer action through multiple mechanisms (Zi & Simoneau, 2005). The basic molecular structure of chalcones include two aromatic rings linked by an unsaturated three carbon bridge. Because of α,β-unsaturated ketones in their structures, chalcones react with thiols instead of amino and

hydroxyl groups, thus less likely to react with nucleic acids and therefore are not associated with mutagenesis as are some other alkylating chemotherapeutics (Zi & Simoneau, 2005; Mahapatra,2015).

1.1.3 Kava-kava toxicity

Kava drinking have been safely used for thousands of years in the South Pacific region with no documented side effects, however from 1999 to 2002 herbal hepatotoxicity was unexpectedly reported in patients worldwide (Showman *et al.*, 2015). Due to these reports, kava was banned in the European Union and Canada, recalled in Australia and included on the USA Food and Drug Administration (FDA) consumer advisory list (Teschke *et al*., 2011, Martin *et al.*, 2014; Showman *et al.*, 2015).

Traditionally kava is prepared extracting compounds from its roots using aqueous solutions, but modern extraction techniques utilizes organic solvents (acetone and ethanol), reaching significantly higher levels of kavalactones and chalcones in the extract (Table 2) (Zhou *et al.*, 2010; Martin *et al.*, 2014). Although it was an important concern about liver injury, toxicity cases occurred after the use of kava aqueous solution in the South Pacific region as well, suggesting that solvents did not play a major role in toxicity (Zhou *et al.*, 2010; Teschke *et al*., 2011; Abu *et al.*, 2013).

Initially, kavalactones have been proposed to account for kava toxicity, but *in vitro* and *in vivo* experiments did not show significant effects (Singh & Devkota, 2003; Zhou *et al.*, 2010). Other compounds of kava preparations, such as flavokawain B were also pointed as toxic constituents, but despite of vigorous research efforts, there is little evidence on this

subject and this affirmation has been refuted for some studies (Teschke *et al*., 2011; Abu *et al.*, 2013).

Flavokawain B, revealed cytotoxicity against hepatoma cells (HepG2) and normal immortalized liver cells (L-02). Also, *in vivo* orally administered FKB (25mg/kg body weight), showed modest signs of hepototoxicity in mice, but in a concentration value 250 times higher than the usual daily uptake by humans (Zhou *et al.*, 2010; Teschke *et al*., 2011; Showman *et al.*, 2015). On the other hand, FKB has also demonstrated hepatoprotective effects (Abu *et al.*, 2013; Pinner *et al.*, 2016).

Table 2: Contents of flavokawain B and total kavalactones in Kava roots extracts (mg/g dried weight) by different extraction solvents

Extract solvent	FKB (mg/g)	Total kavalactones (mg/g)
Water	0.2	46.6
60% acetone	26	474.8
Acetone	33.7	570
95% ethanol	32.3	548.8

Modified from Zhou *et al.*, 2010.

Some concerns were also focused on the possibility that kava raw material could have been contaminated by mould hepatotoxins. Post haverst storage conditions, the warm and humid weather of Pacific, could favor mould proliferation. Moreover, mycotoxins, such as aflatoxins which are potentially toxic to human liver, were encountered in kava preparations, suggesting that kava hepototoxicity cases might be related to contaminations, instead of the kava constituents (Li *et al*., 2008; Teschke *et al*., 2011; Martin *et al.*, 2014).

In summary, the toxicity related to Kava extract intake is controversial and no plausible mechanism for the alleged hepatotoxic effect of Kava has been identified.

1.1.4 Kava-kava and cancer

A number of countries in the South Pacific have very low cancer incidence compared to other parts of the world, despite of the high proportion of smokers in these populations. Considering this, Henderson *et al.* (1985), has proposed that a dietary protective factor might be involved.

Later, Steiner (2000) observed a close inverse relationship between cancer incidence and kava consumption. First, he reported an age-standardized cancer incidence for kava-drinking countries (Vanuatu, Fiji, Western Samoa and Micronesia) to be one fourth to one third the incidence in non-kava drinking countries (USA) and non-kava drinking Polynesians (New Zealand). Steiner (2000) also highlighted an unexpected gender ratio of cancer in the major kava-drinking countries (Vanuatu, Fiji and Western Samoa), where overall cancer incidence is more frequent in women then in men, which only occur in 10 out of 150 cancer incidence reporting locations in the world. These reports are very intriguing, since the majority of kava consumption is performed by men in those regions (Shaver & Sosis, 2014).

Considering the known anticancer properties of chalcones, combined with the epidemiologic data about Kava, researches have been done in order to determine the chemopreventive action of kava-kava compounds against many types of cancers (Abu *et al.*, 2013). Among the kava-kava coumpounds, the chalcones but not the kavalactones, showed cytocidal action against different types of cancer cell lines (Zhou *et al.*, 2010). Between the three flavokawains (FK) encountered in kava extract, FKB showed to be the most potent compound and have been extensively studied (Abu *et al.*, 2013). For this reason, FKB was the subject of our study and will be discussed separated on the next topic.

Flavokawain A (FKA), one of the chalcones of kava extract, was reported to possess anti-inflammatory and anti-cancer activities by suppressing the expression of iNOS and COX-II, through the inhibition of NF-kB pathway in LPS-stimulated macrophage cells (Kwon *et al.*, 2013). Zi and Simoneau (2005) have also shown antitumor effects of FKA against bladder cancer *in vitro* and *in vivo* by involvement of mitochondrial apoptotic pathway. Besides, FKA had antitumor effects against breast cancer cell lines (MCF-7 and MDA-MB231) via intrinsic apoptotic pathway and cell cycle arrest (Abu *et al.*, 2014). It also inhibited tube formation of endothelial cells *in vitro*, demonstrating a potential anti-metastatic action (Abu *et al.*, 2014).

Flavokawain C (FKC) has been tested in bladder and colon cancer cell lines for its anti-cancer activity showing anti-proliferative and apoptotic action as well (Abu *et al.*, 2013; Phang *et al*., 2016).

1.1.5 Flavokawain B

Flavokawain B, scientifically known as *6'-hydroxy-2,4'-dimethoxychalcone*, was found for the first time in the roots of *Piper methystcum.* Later, it was also reported in other species, such as *Aniba riparia*, *P. triangularis var. palloda* and *Didymocarpus corchorijolia* (Wollenweber *et al*., 1981; Kuo *et al.*, 2010; ABU *et al.*, 2013). FKB interacts with several important molecular proteins and signaling pathways, demonstrating anti-inflammatory, anti-nociceptive and anti-cancer properties (Wu *et al*., 2002; Feroz *et al.*, 2012; Abu *et al.,* 2013).

The anti-inflammatory effects of the constituents of kava were accessed by Di Wu *et al*. (2002), where FKB was the most active among the compounds tested, causing

pronounced inhibition of COX-I (77%) and II (16%) enzymes (Wu *et al*., 2002). Lin *et al.* (2009) also found that flavokawain B had an impressive effect in inhibiting nitric oxide production, prostaglandin E2, TNF-α, COX-II and the NF-kB pathway.

The anti-nociceptive activity of flavokawain B was proved by Mohamad *et al.*, (2010), who have demonstrated that intraperitoneal administration of FKB produced markedly dose-dependent suppression of nociceptive responses, both centrally and peripherally mediated. Moreover, compared to acetylsalicylic acid, FKB was 68 fold more effective. These findings might have additional therapeutic implications in the development of a new drug to treat inflammatory pain (Mohamad *et al.*, 2010; Mohamad *et al.*, 2011).

The anticancer properties of Flavokawain B have been demonstrated in several cancer cell lines, such as osteosarcoma, oral carcinoma, synovial sarcoma, prostate, colon and lung cancers, between others. Table 3 summarizes the *in vitro* half maximal inhibitory concentration (IC_{50}) of Flavokawain A, B and C in selected cell lines according to the available publications.

Table 3: Half maximal inhibitory concentration (IC_{50}) of Flavokawain A, B and C in selected cancer cell lines according to the available publications

Flavokawain	Cancer type	Cancer cell line	IC_{50} (μM)	Treatment (hours)	Reference
FKA	Bladder	T24	16.7	48h	Zi & Simoneau, 2005
		RT4	20.8	48h	Zi & Simoneau, 2005
		EJ	17.2	48h	Zi & Simoneau, 2005
	Liver	HepG2	62.38	24h	Li *et al*., 2008
	Breast	MCF-7	25	72h	Abu *et al.*,2014
		MDA-MB231	17.5	72h	Abu *et al.*,2014
					Abu *et al.*,2014
FKB	Bladder	T24	6.7	48h	Zi & Simoneau, 2005
		RT4	15.7	48h	Zi & Simoneau, 2005
		EJ	5.7	48h	Zi & Simoneau, 2005
	Oral epidermal carcinoma	KB	~70	24h	Lin *et al.*, 2012
	Breast	4T1	47.5	72h	Abu *et al*., 2015
	Cervix	Ca Ski	109	48h	Abu *et al.*, 2013
	Colon carcinoma	HCT 116	~25	24h	Kuo *et al.*, 2010
	Lung adenocarcinoma	A549	~50	24h	Kuo *et al.*, 2010
	Lung carcinoma	H460	18.2	48h	An *et al*., 2012
	Prostate cancer	LAPC4	32	48h	Tang *et al.*, 2010
		LANCaP	48.3	48h	Tang *et al.*, 2010
		PC-3	6.2	48h	Tang *et al.*, 2010
		DU145	3.9	48h	Tang *et al.*, 2010
		22RV1	58.4	72h	Li *et al.,* 2012
		C4-2B	7.7	72h	Li *et al.,* 2012
	Oral squamous carcinoma	HSC-3	17.2	24h	Hseu *et al.*, 2012
		Cal-27	26.7	24h	Hseu *et al.*, 2012
	Melanoma	A-2058	18.3	24h	Hseu *et al.*, 2012
	Synovial sarcoma	SYO	10	72h	Sakai *et al.*, 2012
		HS-SY-II	21	72h	Sakai *et al.*, 2012
	Adenoid cystic carcinoma	ACC-2	4.69	48h	Abu *et al.*, 2013
	Uterine Leiomyosarcoma	SK-LMS-1	~3.3	72h	Eskander *et al.*, 2012
	Endometrial adenocarcinoma	ECC-1	~4.4	72h	Eskander *et al.*, 2012
	Osteosarcoma	143B	~6.9	72h	Ji *et al*, 2013
		OS160	~19	72h	Ji *et al*, 2013
		MG-63	~13	72h	Ji *et al*, 2013
		Saos-2	~26	72h	Ji *et al*, 2013
	Liver	L-02	35.15	24h	Li *et al.,* 2008
		HepG2	62.38	24h	Li *et al.,* 2008
FKC	Bladder	EJ	14.6	48h	Abu *et al.*, 2013
		T24	10.6	48h	Abu *et al.*, 2013
	Liver	Hep G2	59.48	48h	Li *et al*., 2008

Modified from Abu *et al.*, 2013.

These studies have also determined normal tissue cells viability upon treatment with FKB in order to analyze toxicity. A more pronounced action of FKB was observed against

cancer cells. Table 4 summarizes the *in vitro* IC_{50} of Flavokawain B towards normal cell lines already tested.

Table 4: Half maximal inhibitory concentration (IC_{50}) of Flavokawain B in selected normal cell lines according to the available publications

Tissue type	Cell line	IC_{50}(µM)	Time of treatment (h)	Reference
Human fibroblasts	NIH3T3	~25	24h	Kuo *et al.*, 2010
Human fibroblasts	HFW	25 – 50	24h	Kuo *et al.*, 2010
Prostate epithelial	PrECs	Not reached (>17.6 µM)	48h	Tang *et al.*, 2010
Prostate stromal	PrSCs	Not reached (>17.6 µM)	48h	Tang *et al.*, 2010
Human endometrium fibroblasts	T-HESC	Not reached (>35.,2µM)	72h	Eskander *et al.*, 2012
Human gengival fibroblasts	HGF	30 – 40	72h	Lin *et al,* 2012
Murine macrophage	RAW 264.7	Not reached (>40 µM)	24h	Lin *et al*, 2009
Liver	L-02	35	48h	Zhou *et al*, 2010

The antiproliferative and cell death mechanisms involved in the exposition of different cancer cells to FKB have shown similar pathways, such as the activation of apoptosis and cell cycle arrest (Zi & Simoneau, 2005; Li *et al*., 2008; Kuo *et al.*, 2010; Tang *et al.*, 2010; Zhou *et al.*, 2010; An *et al.*, 2012; Eskander *et al.*, 2012; Hseu *et al.*, 2012; Li *et al.,* 2012; Lin *et al.*, 2012; Sakai *et al.*, 2012; Ji *et al.*, 2013; Kwon *et al.*, 2013; Abu *et al.*,2014, Abu *et al*., 2015). Figure 4, modified from HSEU *et al.*, (2012), illustrates and summarizes the possible mechanisms of FKB against different cancer cells according to the available publications.

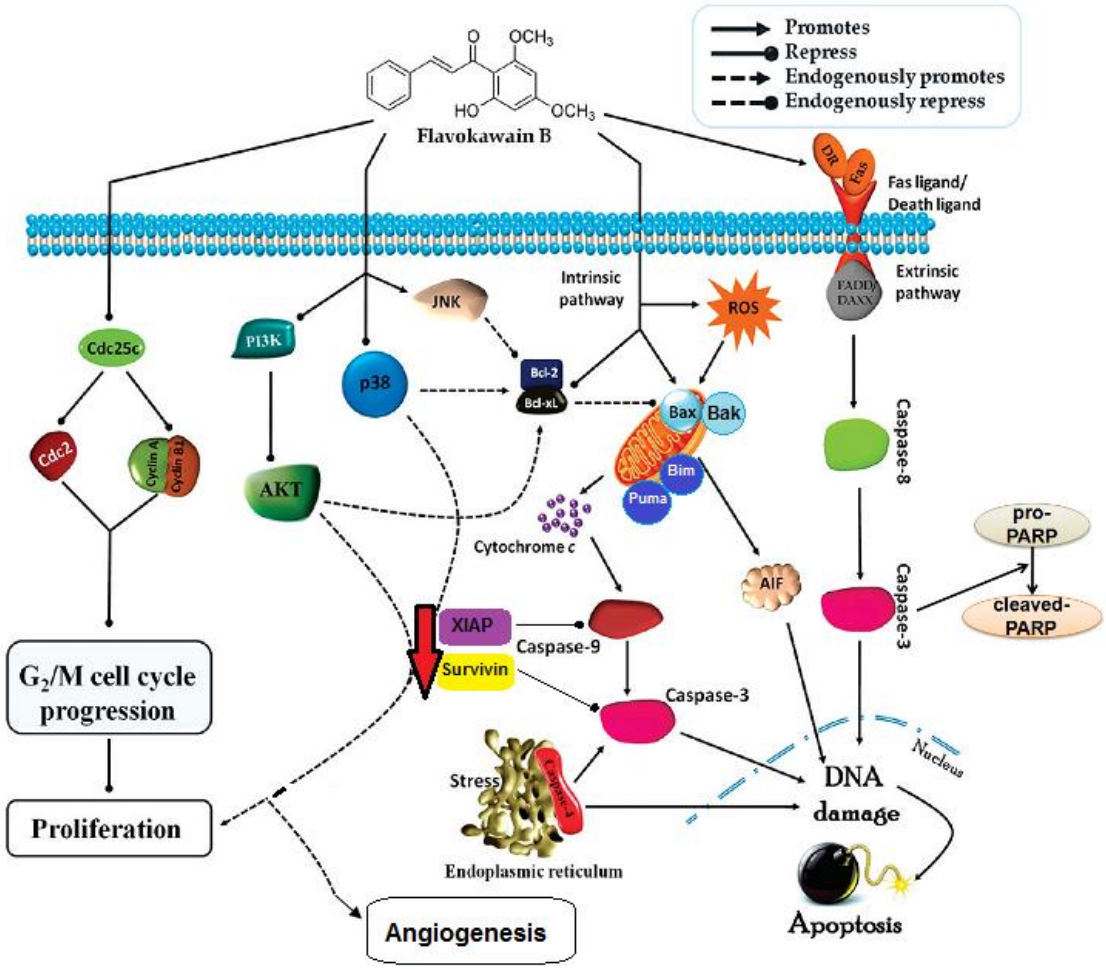

Figure 4: Proposed diagram of FKB induced G_2/M arrest, apoptosis and Akt/p38 MAPK inactivation of different cancer cells.
Modified from Hseu *et al*., 2012.

Flavokawain B apoptotic action was demonstrated through typical apoptotic cell morphology (cell membrane blebbing, shrinkage, nuclear condensation and fragmentation) and activation of the intrinsic and extrinsic apoptotic pathways with upregulation of caspase 8, 9, 3/7, cleavage of PARP and upregulation of the death receptor 5 (DR5). These observations and further studies implied that death receptor and mitochondrial-mediated apoptotic pathways were involved. Altered mitochondrial membrane permeabilization, release of cytochrome C, upregulation of DR5, Bim, Puma, Bax, Bak and downregulation of anti-apoptotic proteins (Bcl-2, XIAP and surviving) were also reported in several cancer cell

lines (Kuo *et al.*, 2010; Tang *et al.*, 2010; An *et al.*, 2012; Lin *et al.*, 2012). Moreover, it was also observed that flavokawain B induced a G2/M arrest, involving important cyclin/cdk complexes (Eskander *et al.*, 2012; Lin *et al.*, 2012). The PI3K/Akt signaling pathway is implied in cell proliferation, survival, cell-cycle control, angiogenesis and others. FKB treatment of human oral carcinoma cells (HSC-3) inhibited the activation of Akt by a decrease on its phosphorylation (Figure 4) (Hseu *et al.*, 2012).

Further studies *in vivo* with nude mice have shown that flavokawain B significantly reduced tumor growth in xenograft models of prostate, human squamous carcinoma and breast cancers (Tang *et al.*, 2010; Li *et al.,* 2012; Lin *et al.,* 2012; Abu *et al*., 2015).

FKB can also be a promising anti-metastatic drug, since it inhibited the expression of matrix-metalloproteinase 9 (MMP-9) and urokinase plasminogen activator in oral epidermal carcinoma cells (KB) and apparently reduced angiogenesis in tumors of a xenograft model (Lin *et al.*, 2012). Abu *et al.* (2015) demonstrated in a xenograft model of breast cancer, that the oral treatment with FKB reduced tumor growth and the levels of angiogenesis related proteins (Abu *et al.,* 2015). Moreover, very recently, Abu *et al*. (2016), have shown that FKB inhibited cell migration of breast cancer cells, impaired endothelial tube formation *in vitro* and regulated several metastasis related proteins, such as VEGF, SNAIL and CXCR4. However, the anti-angiogenic potential of FKB, was poorly studied and has not been demonstrated *in vivo* until now.

1.2 Ovarian cancer

1.2.1 Epidemiology

Ovarian cancer is the second most common malignancy of the female genital tract in developed countries and the third most common in developing countries, where cervical cancer incidence is still high (Chen & Berek in UpToDate, 2016). It represents the greatest clinic challenge in gynecology oncology, due to the lack of obvious clinical signs and symptoms, specific methods for early detection and its high mortality rates (Ramalingam, 2016). For all stages, the 5-year survival rate is 45%, but most of patients are diagnosed with advanced disease reaching around 30% survival rate in 5 years. (Chien *et al.*, 2007).

The estimated annual incidence of this disease worldwide is over 200,000 cases, with around 125,000 annual deaths (Siegel *et al*., 2014). The number of new cases is usually greater in high than in middle- to low-income countries. Age-standardized incidence is 11.7 per 100,000 in the UK, 8.0 per 100,000 in the USA and 5.2 per 100,000 in Brazil (Ramalingam, 2016). According to the Instituto Nacional de Câncer (INCA) database, in Brazil there were 3.283 deaths related to ovarian cancer in 2013 and around 6150 new cases are estimated for 2016 (INCA database <www.inca.gov.br>).

1.2.2 Pathology of epithelial ovarian cancer

The origin and pathogenesis of epithelial ovarian cancer (EOC) have long been investigated but is still poorly understood. Traditionally, two main hypotheses were proposed: incessant ovulation and persistent exposure to gonadotropins, both leading to malignant transformation of the ovarian epithelium (Kurman & Shih, 2010; Ramalingam,

2016). However, based on the detection of serous tubal intraepithelial carcinomas (STIC) and its molecular patterns, it has also been proposed that the fallopian tube might be one EOC site of origin (Kurman & Shih, 2010; Sorensen *et al.,* 2015). The risk and protective factors that have been related to epithelial ovarian cancer are listed on Table 5 (Sorensen *et al.,* 2015; Chen & Berek in UpToDate, 2016).

Table 5: Risk and protective factors of ovarian cancer

Risk Factors	**Protective Factors**
Age > 50 years old	Oral contraceptives
Infertility	Multiparity
Early menarche and late menopause	Salpingo-oophorectomy
Nuliparity	Tubal ligation
Endometriosis	Hysterectomy
Polycystic ovarian syndrome	Breastfeeding
Postmenopausal hormone therapy	
Genetic Factors : BRCA 1/2 mutations	
Lynch syndrome	
Family history of breast and ovarian cancer	
Environmental factors: Smoking	
Diet	
Sedentarism	
Obesity	

Chen & Berek in UpToDate, 2016. Available at <www.uptodate.com>, accessed on March 26, 2016.

In the past, ovarian carcinoma has been considered to be one single disease; however studies have shown that it is a heterogeneous pathology that comprises a variety of tumors with various histopathological and genomic features with different biological behavior (Bai *et al.*, 2016). The most lethal and the majority of ovarian malignancies (90% percent) are of epithelial origin, the reminder histology types arise from other ovarian cells, such as germ cell tumors and sex cord-stromal tumors. Epithelial ovarian cancer is subdivided into serous, mucinous, endometrioid, clear cell and transitional cell tumors.

Serous carcinomas are the most frequent category (~50%) and are separated into low and high grade based on the degree of nuclear atypia and mitoses (De Picciotto *et al.*, 2016).

Kurman & Shih (2010), have proposed a dualist model, recently revised and expanded by the same authors (Kurman & Shih, 2016), that categorizes various types of epithelial ovarian cancer into two groups based on their histology, molecular biology and natural history (Figure 5) (Kurman & Shih, 2010; Kurman & Shih, 2016).

Type I tumors are clinically indolent and present usually at low stage. They consist of low-grade serous, endometrioid, clear cell, seromucinous, mucinous carcinomas and malignant Brenner tumors. These tumors often demonstrate mutations in *KRAS, BRAF, PIK3CA, ERBB2* or *PTEN* (Kurman & Shih, 2016). When confined to the ovary type I tumors have an excellent prognosis, but advanced stage tumors have a poor outcome and usually do not respond well to chemotherapy (Kim *et al.*, 2012). On the other hand, type II tumors are highly aggressive and almost always are diagnosed in advanced stage (>75%) with extraovarian disease at the peritoneum and omentum, accompanied by ascites (Kurman & Shih, 2010). They include high-grade serous, carcinosarcomas and undifferentiated carcinomas that are frequently associated with mutations in *TP53, BRCA1, BRCA2, NF1* and other homologous recombination repair genes. Extended surgery and chemotherapy have improved progression free survival (PFS) and, to a very modest extent, the overall survival, but most of the patients with type II tumors have recurrences and die because of disease progression (Kim *et al.*, 2012; Kurman & Shih, 2016).

These findings suggest that the different types of epithelial ovarian cancers develop along distinct molecular pathways and should be also accessed differently. Figure 5

represents the dualistic model of ovarian cancers proposed by Kurman & Shih (2016) and its molecular alterations.

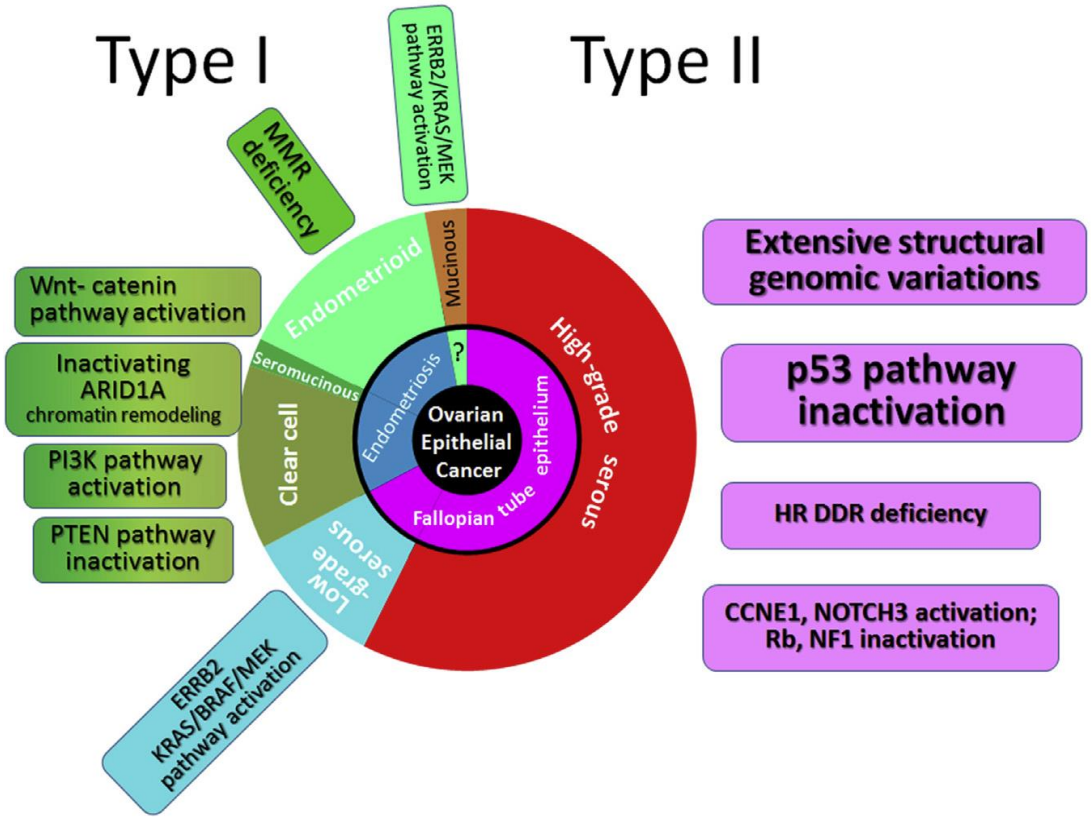

Figure 5: Expanded dualist model of ovarian carcinogenesis and its molecular pathways. Type I carcinomas comprise, low-grade serous, clear cell, endometrioid and mucinous carcinomas. Type II include mainly high-grade serous carcinomas. The inner circle indicates the probable origin of neoplasms and the molecular alterations of each tumor are indicated in the square boxes (Reproduced from Kurman & Shih, 2016).

1.2.3 Treatment and new perspectives

Current management of ovarian cancer in general is based on radical surgery consisting of total abdominal hysterectomy, bilateral salpingo-oophorectomy, omentectomy, peritoneal washings and pelvic lymph node sampling, together with chemotherapy. However, in the last 50 years, there has been only marginal improvement in 5 years overall survival (Coward *et al.*, 2015).

Over the years experts have explored different combinations of antitumor drugs in order to improve the prognosis of ovarian cancer. In 1976, cisplatin reported efficacy in ovarian cancer an initiated the use of combination chemotherapy. In 1980 paclitaxel, constituent of the Pacific Yew tree, *Taxus brevifolia*, showed great activity in EOC, becoming part of the first line therapy. Afterwards, carboplatin, a cisplatin analogue, was reported to have fewer side effects and replaced cisplatin. The carboplatin-paclitaxel combination is now the most universal regimen in the treatment of epithelial ovarian cancer (Kim *et al.*, 2012; Della Pepa *et al.*, 2015). Further improvements have been sought in order to increase the efficacy of first-line chemotherapy, such as delivering drugs through the intraperitoneal (IP) route (Jaaback & Johnson, 2005). Although the IP therapy prolonged survival compared to the intravenous (IV) administration, there were significantly higher side effects and in many countries the IV chemotherapy is still preferred (Armstrong *et al.*, 2006).

Despite the activity of first-line chemotherapy, which gives response rates up to 80%, the majority of patients die of the recurrent resistant disease and it has not substantially changed overall survival in more than 50 years (Armstrong *et al.*, 2006; Kim *et al.*, 2012; Coward *et al.,* 2015). The strongest independent variable in predicting survival is still residual macroscopic disease after surgery, suggesting that novel regimens of chemotherapy, based on molecular pathogenesis of ovarian cancer are urgently needed (Kim *et al.*, 2012).

Molecular-targeted therapies, alone or in combination with chemotherapy, have produced promising results in preclinical and clinical studies (Borley & Brown, 2015; Coward *et al.,* 2015; SCOTT *et al.*, 2015; Wang & Siqing, 2015). The most explored pathways are:

phosphatidylinositide 3-kinase (PI3K) and Poly (adenosine diphosphate [ADP]-ribose) polymerase (PARP) inhibitors, besides antiangiogenic drugs.

1.2.3.1 PI3K pathway inhibitors

PI3K-AKT-mTOR is a complex signaling pathway altered in many types of cancers that coordinates a number of upstream inputs, such as growth factors and tyrosine kinase receptors. Its stimulation causes activation of a cell surface receptor and phosphorylation of PI3K (Engelman, 2009). Activated PI3K then phosphorylates lipids on the plasma membrane, forming the second messenger phosphatidylinositol (3,4,5)-trisphosphate (PIP_3). As a result, the PI3K complex is recruited to the plasma membrane and activates the pyruvate dehydrogenase kinase 1 (PDK1) and Akt proteins. On the other hand, the phosphatase and tensin (PTEN) analog protein acts as an endogenous pathway repressor by de-phosphorylating PIP3 back to PIP2 (Engelman, 2009; Dobbin & Landen, 2013; Cheaib *et al*., 2015).

Akt is a serine-threonine kinase that is activated through phosphorilation of both residues: threonine 308 (Thr308) and serine 473 (Ser473) (Vincent *et al.*, 2011). It regulates a large number of downstream targets related to cellular survival and metabolic processes, such as the transcription of anti-apoptotic genes (X-linked inhibitor of apoptosis protein [*XIAP*], *Bcl-2* and *surviving*), oncogenes (p53) and nuclear factor-kB (NF-kB). Akt also promotes cell cycle progression and increases the expression of genes involved in angiogenesis, such as the vascular endothelial growth factor (*VEGF*) (Figure 6) (Engelman, 2009; Vincent *et al.*, 2011; Leary *et al.*, 2013; Cheaib *et al.*, 2015).

Activation of the PI3K-AKT-mTOR signaling cascade occurs frequently in epithelial ovarian cancer and mediates cell-cycle progression, cell survival, migration, invasiveness and angiogenesis (Wang & Fu, 2015). This pathway is up-regulated in a significant proportion of ovarian cancers via either direct upstream stimulation (growth factor receptors and their ligands), indirect activation via cross-talk with the Ras pathway, intrinsically activating genetic alterations of PI3K/Akt or via loss of function in the tumor suppressor gene PTEN (Engelman, 2009). Moreover, ovarian cancer cells that either overexpress active Akt/AKT1 or gene amplification of AKT2 are more resistant to chemotherapy (Bai *et al*, 2016). Therefore, this pathway is an attractive candidate for therapeutic interventions against EOC and inhibitors targeting it are in various stages of pre-clinical development with promising results, such as, Perifosine (Akt inhibitor) and Temsirolimus (mTORC1 inhibitor) (Dobbin & Landen, 2013; Leary *et al.*, 2013).

Figure 6 illustrates the PI3K-AKT-mTOR signaling pathway alterations with its implications in ovarian cancer, such as increased expression of anti-apoptotic and angiogenic genes, besides stimulation of cell cycle progression.

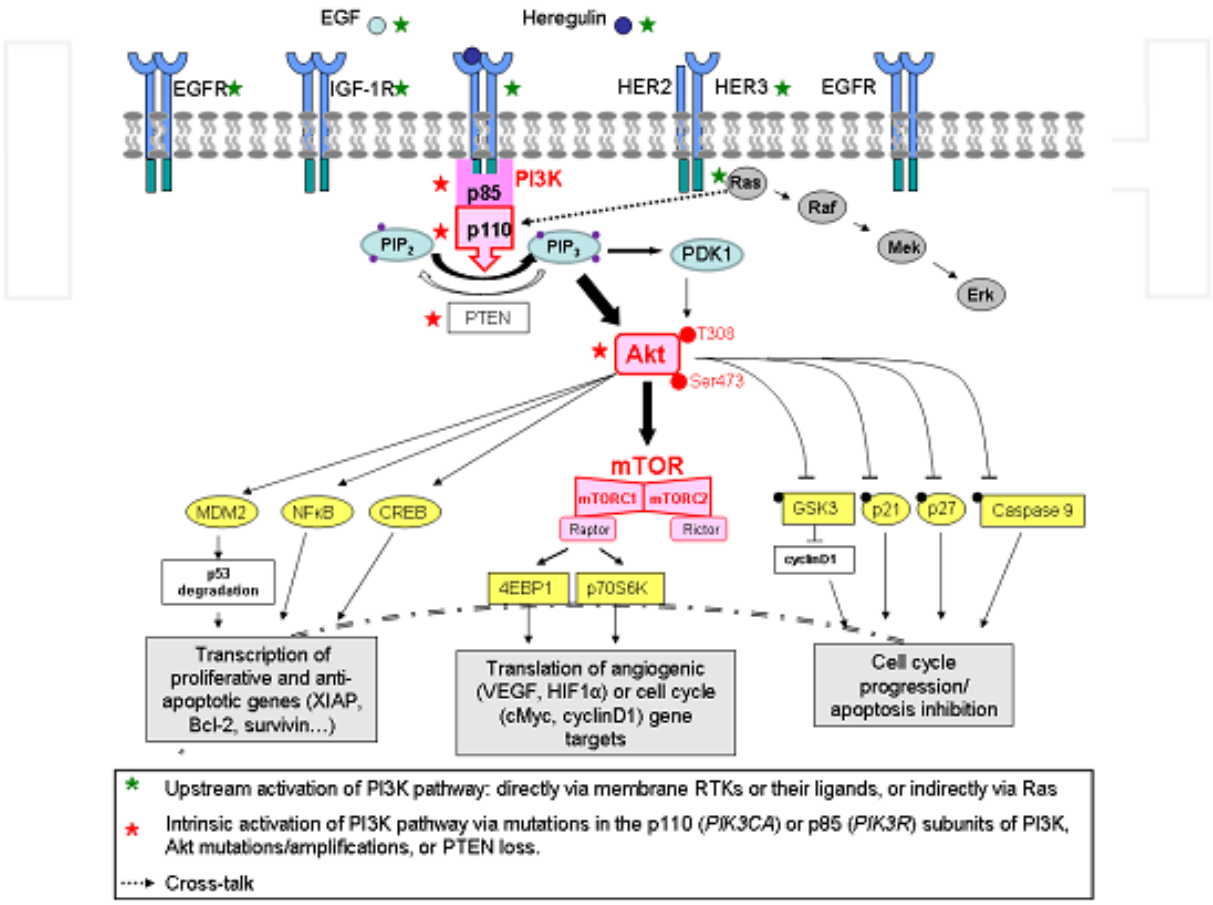

Figure 6: The PI3K/Akt/mTOR signaling pathway, frequently up-regulated in ovarian cancer
(Reproduced from Leary *et al.*, 2013)

1.2.3.2 PARP inhibitors

PARP enzymes play a vital role in cellular DNA repair, coordinating base-excision repair pathways. Inhibition of PARP causes accumulation of single-strand brakes, which causes double-strand breaks during replication. These defects are usually corrected by homologous recombination proteins, such as BRCA 1 and 2. When *BRCA* gene is mutated, the inhibition of PARP causes genomic instability and cell death (De Picciotto *et al.*, 2016).

Females who carry *BRCA1* and *BRCA2* alterations are at high risk of developing ovarian cancer, with lifetime risks of 16 to 64% (Friedman *et al.*, 2005; Schayek *et al.*, 2015).

BRCA mutated patients seem to be particularly sensitive to PARP inhibitors alone and in combination with chemotherapy, especially in relapsed platinum-sensitive high grade serous disease (Scott *et al.*, 2015; De Picciotto *et al.*, 2016; NCCN, 2016). These data implicated in the approval of Olaparib, a PARP-1, -2 and -3 inhibitor, by the FDA, limited to the *BRCA1/2* mutation carriers. It was the first biologic agent to treat ovarian cancer based upon personalized medicine (Wang & Fu, 2015). Many trials are still being done with Olaparib and other PARP inhibitors in association with different biologic agents in order to enhance effectiveness. Because of the significant impact on cancer therapy, the *BRCA1/2* status screening is now recommended for all patients diagnosed with high grade serous ovarian cancer (HGSOC) independently of the family history of breast and ovarian cancers (Scott *et al.*, 2015; NCCN, 2016).

1.2.3.3 Antiangiogenic drugs

Cancer has the ability to spread to adjacent or distant organs, what makes it life threatening. Angiogenesis, one of the hallmarks of cancer, is required for tumor growth beyond 1-2mm, being essential for tumor invasion and metastasis (Hanahan & Weinberg, 2011; Weis & Cheresh, 2011). Neovascularization requires the recruitment of vasculature, circulating endothelial cells and signals of pro-angiogenic mediators, such as VEGF (Hanahan & Weinberg, 2011; Eskander & Tewari, 2014).

Metastatic intra-peritoneal dissemination of ovarian cancer relies on the ability of floating cells to survive, proliferate and metastasize. Animal models have shown the ability of intra-peritoneal ovarian cancer cells to attach to avascular areas and form vascular deposits (Leinster *et al.*, 2012; Eskander & Tewari, 2014). Moreover, approximately 97% of

ovarian tumors overexpress the VEGF ligand and this expression correlates with ascites formation, poor prognosis and reduced survival (Kim *et al.*, 2012; Colombo *et al.*, 2016). For these reasons, neovascularization is thought to be particularly crucial in the persistence of ovarian cancer and has been a target of clinical research (Eskander & TewarI, 2014; Wang & Fu, 2015).

Therapies targeting angiogenesis are currently being investigated, with promising results against EOC, both as single agents as well as in combination with chemotherapy (Coward *et al.,* 2015). Monoclonal antibodies against VEGF-A or Tie-2 receptor – Bevacizumab and Trebananib – have shown to prolong progression-free survival (PFS) in patients with recurrent disease (Colombo *et al.*, 2016). Bevacizumab is the most investigated and promising molecular target drugs in ovarian cancer, being able to neutralize all major isoforms of VEGF, prevent endothelial cell proliferation and vessel formation (Gadducci *et al.*, 2015; Colombo *et al.*, 2016). Phase III clinical trials have already demonstrated that Bevacizumab combined with chemotherapy provides a statistically and clinically significant improvement in PFS in the primary and recurrent advanced ovarian cancer (Colombo *et al.*, 2016).

Taken together, the described anticancer potential of Flavokawain B combined with the urgently need of new therapy approaches for ovarian cancer have prompted us to investigate the FKB action towards ovarian cancer cells and better characterize its antiangiogenic potential.

2 OBJECTIVES

- Investigate the potential of FKB as a new additional drug in the treatment of ovarian cancer.

- Examine the cytocidal effect of Flavokawain B against OVCAR-3 cells with different concentrations and time of drug exposure.

- Analyze the effect of Flavokawain B against normal cells (human fibroblasts) and compare it to its action against cancer cells.

- Determine the half-maximal inhibitory concentration (IC_{50}) *in vitro* of FKB over OVCAR-3 cells and fibroblasts.

- Investigate the possible mechanisms of action by which Flavokawain B causes cancer cells death.

- Evaluate the Flavokawain B action over the activation of the Akt pathway.

- Better characterize the antiangiogenic potential of Flavokawain B *in vitro* utilizing Human umbilical endothelial cells (HUVEC) and Human brain microvascular endothelial cells (HBMEC).

- Demonstrate the antiangiogenic action of Flavokawain B *in-vivo* utilizing a Zebrafish angiogenesis model.

3 MATERIALS AND METHODS

3.1 Drug

Flavokawain B powder was purchased from the LKT Laboratories, Inc. (Product ID: F4503) and diluted in DMSO at 5mg/mL stock solution.

3.2 Cell Lines

OVCAR-3: Human ovary ephitelial adenocarcinoma cell line was purchased from Banco de células do Rio de Janeiro (BCRJ) – Lote: 0507708. This cell line has been established from the malignant ascites of a 60 years old caucasian patient with progressive adenocarcinoma of the ovary, resistant to combination chemotherapy with cyclophosphamide, adriamycin and cisplatin. It is an aneuploid cell line, with chromosome counts in the sub to near-triploid range and has *TP53* missense mutations described.

HUVEC: Human umbilical vein endothelial cells were purchased from Life Technologies – GIBCO (Cat# C-003-5C).

HBMEC: Human brain microvascular endothelial cells from ATCC collection (ATCC, USA) were obtained from Dr. Hanna Caldas, laboratory of the Neuro-oncology department at Wake Forest Baptist Medical Center (North Carolina, USA).

HUMAN FIBROBLASTS: Human skin fibroblasts were established from a skin biopsy of a healthy anonymous donor who voluntarily accepted to contribute with the research. The volunteer has signed a free and clarified consent term. The procedure has been approved by the research ethics committee – COEP (0434.0.203.000.10).

3.3 Cell culture conditions and compounds

The OVCAR-3 and HBMEC cells were cultured in RPMI medium containing 10% fetal bovine serum (FBS); HUVEC cells were cultured in M200 basal media, supplemented with Large Vessel Endothelial Supplement (LVES) and Fibroblasts were grown in DMEM with 10% FBS. All culture media used were supplemented with 1% penicillin-streptomycin solution.

Cells were grown at 37^{o}C in 5% CO_2 incubator using T75 flasks and 100mm dishes (SARSTEDT AG & Co, Nümbrecht Germany). All the cell culture procedures were done with aseptic conditions under a laminar flow hood. The cells were monitored under an inverted microscope Axiovert 25 (Carl Zeiss, Germany). All the cell culture reagents listed were purchased from Life Technologies (Carlsbad, USA) or Sigma-Aldrich Co. (St. Louis, CA, USA).

3.4 Antibodies

The antibodies utilized and their respective providers are listed on the following table:

Table 6: List of antibodies utilized for Western-Blotting

Antibodies	**Catalog Number**	**Provider**
Anti-Actin (C4)	#MAB1501	Millipore
Anti -Bcl-2	#2872S	Cell Signalling Technology
Anti-Bcl-X_L(H-5)	#sc-8392	Santa Cruz Biotechnology
Anti- AKT1	#13038S	Cell Signalling Technology
Anti-pAKT	**#**75692	Cell Signalling Technology
Anti-BAX (p19)	#sc-7480	Santa Cruz Biotechnology
Anti-BAK (G-23)	#sc-832	Santa Cruz Biotechnology
Anti-AIF (H300)	#sc55519	Santa Cruz Biotechnology
Anti-IgG-Mouse	#7076	Cell Signalling Technology
Anti-IgG-Rabbit	#7074	Cell Signalling Technology

3.5 Primary fibroblasts culture

Primary fibroblast culture was established as described by MARTINS, 2015. A skin sample of 3mm from the forearm was obtained with a disposable punch, commonly utilized for dermatology biopsies. The biopsy procedure was performed by a trained doctor after local antisepsis and under local anesthesia. Immediately after, the skin sample was kept in DMEM (Dulbecco's modified Eagle's medium -High Glucose) supplemented with 10% FBS, 2% penicillin/streptomycin, 1% amphotericin B and 1% sodium pyruvate at 37^0C until the moment of culture. All the cell culture reagents listed were purchased from Life Technologies (Carlsbad, CA, USA) or Sigma-Aldrich Co. (St. Louis, MO, USA).

The skin sample was divided into smaller pieces and transferred to two 100mm cell + dishes (SARSTEDT AG & Co, Nümbrecht Germany). The fragments were covered with microscopy coverslips sterilized. It was added 10mL of DMEM high glucose supplemented with 10% FBS, 1% penicilin/streptomycin and 1% sodium pyruvate at 37^oC. The biopsies were kept at 37^oC in 5% CO_2 incubator and not manipulated for three days. Cell growth was monitored using an inverted microscope Axiovert 25 (Carl Zeiss, Germany) and the culture media was changed twice a week. The coverslips were taken from the dishes after a significant number of fibroblasts were visualized. The cells were grown until a confluence of 60 to 70% and splitted into new dishes. The experiments were done with the p1 to p4 cell passages.

3.6 Evaluation of cell and nuclear morphology by light and fluoresce microscopy

To evaluate OVCAR-3 cells morphology and viability after treatment with FKB, cells were analyzed by light and fluorescence microscopy after double staining with 4,6-diamidino-2-phenylindole (DAPI) and Propidium Iodide (PI). DAPI is a fluorescent stain that strongly binds to cell DNA and can pass through an intact cell membrane. PI is also a fluorescent agent that binds to nuclei acids, however is cell membrane impermeant, just being able to stain dead cells after membrane disruption.

Cells were cultivated in coverslips previously coated with Poly-L-lysine and treated with FKB at 5, 10 and 20µg/mL or DMSO 0.1% as a control. After 24 hours of treatment cells were double stained with 7µmol/L of Propidium Iodide (PI) and 300 nM DAPI for 30 min. The cells were washed for 15 min in 2 mL of Phosphate Buffer Saline (PBS) and the coverslips with the attached cells were carefully adapted to a microscopy perfusion chamber covered with PBS at 37^{o}C. Cells were then examined by light and fluorescence microscopy (Carl Zeiss, Germany) with two filters (DAPI fluorescent filter, excitation 340–380 nm, barrier filter 430 nm and a rhodamine filter, excitation 530–560 nm, barrier filter 580 nm). The objectives were used with oil immersion at a 40 magnification. Cells nuclei showed blue fluorescence of DAPI and dead cells were indicated by the red fluorescence of PI. The images were acquired using an Axiovert Zeiss 200 M (Zeiss, Oberkochen, Germany) and for each treatment condition, three microscopic fields were photographed. Adobe Photoshop 6® software was used to merge images of DAPI and PI staining.

3.7 Cell viability MTT assay

The MTT (3-(4,5-dimethylthiazol-2-yl)-2,5-diphenyltetrazolium bromide) is a colorimetric assay for assessing cell viability. MTT is a yellow tetrazolium salt that is reduced to purple formazan crystals by the mitochondrial succinate dehydrogenase enzyme in living cells. Correlation between production of formazan and cell number has been shown (Denizot & Lang *et al.*, 1986; Vistica *et al*., 1991). Afterwards, a solubilizing solution (usually dimethyl sulfoxide) is added to dissolve the insoluble purple formazan product into a colored solution and the absorbance quantified by spectrophotometry**.**

In the present study, OVCAR-3, human fibroblasts and HUVEC cells were plated at a density of 7.5 x 10^3 cells per well in 96-well culture plates (SARSTEDT AG & Co, Nümbrecht Germany) in their respective cell medium containing 10% FBS. After 24 hours, the medium was treated with DMSO 0.1% vehicle control or FKB at different concentrations for 24 and 48 hours. After treatment, MTT reagent was added to the wells at a final concentration of 1mg/mL and incubated at 37^{o} C for 3 hours. After the incubation period, cell media was carefully taken to preserve the formazan crystals and DMSO was added to dissolve then into a purple solution. The absorbance was determined at 595nm using Victor™ X4 (Perkin Elmer Inc., Whaltam, MA, USA) microplate reader. The number of viable cells was evaluated by uptake and reduction of MTT comparing the treated cells to the control group. All experiments were performed at least in triplicate on three separate occasions. Data are presented as mean ±SD.

3.8 Flow cytometry assay

OVCAR-3 cells at 70 to 80% were harvest and $1x10^5$ cells were seeded in 6well plates (SARSTEDT AG & Co, Nümbrecht Germany) overnight. The cells were then treated with 0.1% DMSO or 5, 10 and 20ug/mL of FKB for 24 hours. Afterwards, cells were collected into 2mL tubes and centrifuged for 5 minutes at 400g. The pellet was then resuspended in 1X Binding Buffer and stained with Annexin V and 7-aminoactinomycin D (7-AAD) for 15 minutes according to the manufacturer's protocol (BD Pharmingen™). All analyses were done using appropriate scatter gates to exclude cellular debris and aggregated cells. The stained cells were acquired using FACScanto flow cytometer (BD).

3.9 Western Blotting analysis

Cells were plated at a confluence of $1x10^6$ cells per 100mm plate (SARSTEDT AG & Co, Nümbrecht Germany) and permitted to adhere overnight at 37^oC. After incubation, cells were treated with DMSO 0.1% as a control or 2.5; 5.0; 7.5 and 10ug/mL of FKB for 24 hours. After treatment, cells were harvest and lysed in Lysis Buffer containing: Sodium Fluoride 50 mM, Sodium Orthovanadate 1 mM, 1% Triton X100 and protease inhibitors (AEBSF 104 mM; aprotinina 80 µM; bestatina 4 mM; E-64 110 1,4 mM; leupeptina 2 mM e pepstatina A 1,5 mM).

Protein quantification was performed according the Bradford technique described in 1976 (Bradford, 1976). Between 1,0 to 2,0 µL of protein extract was added to the Bradford (Sigma-Aldrich Co., St. Louis, MO, USA) reagent using 96well-plates (SARSTEDT AG & Co, Nümbrecht Germany). The absorbance was determined using a microplate reader (Victor™

X4) at 595nm. For each quantification procedure, a standard curve with serum albumin (0.2 to 2.0 µg) was utilized.

Volumes of clarified protein lysates containing the same amount of protein (30ug) were electrophoretically resolved on denaturing SDS-polyacrylamide gel 12%, transferred to nitrocellulose membranes, blocked with serum albumin solution for 1 hour and probed with primary antibodies overnight. Proteins were revealed using horseradish peroxidase-conjugated anti-mouse or anti-rabbit antibodies, incubated with ECL Plus kit (GE, Fairfield, CA, USA) and visualized by the enhanced chemiluminescense detection system ImageQuant 400 (GE, Fairfield, CA, USA). The desitometric analysis of the bands was performed using the ImageJ software (National Institutes of Health, USA).

3.10 Live cell microscopy

Time lapse microscopy was utilized to observe tube formation assay of HBMEC cells. $1x10^5$ cells were seeded in a 100mm dish coated with Matrigel® and 15ng/mL of VEGF was added to the cell media. DMSO 0.1% was added to the control dish and 5µg/mL of FKB was added to the treated dish. Cells were placed inside a transparent incubator at 37^oC and 5% CO_2 for 8 hours. Multiple microscope images sequences were recorded using a FV1200 microscope. The images were then viewed at a greater speed and a time-lapse movie was produced. This experiment was performed in Dr. Hanna Caldas laboratory at the Neuro-oncology Department of Wake Forest Baptist Medical Center (North Carolina, USA).

3.11 Tube formation assay

Tube formation assay was performed using the Angiogenesis Starter Kit® (Life Technologies, GIBCO) and according to the manufacturer protocol. A 24well-plate (SARSTEDT AG & Co, Nümbrecht Germany) was coated with 200µl of Geltrex® Matrix solution and incubated at 37^{o}C for 30 minutes to allow the matrix to solidify. Gently 5x10^{4} HUVEC cells were seeded into each well with 0.1% DMSO or 1, 2.5 and 5.0 ug/mL of FKB and incubated for 18 hours at 37^{o}C in a humidified atmosphere of 5% CO_2. At the end of the incubation period, cells were photographed with a digital camera attached to a stereomicroscope (SMZ 1500 Nikon) with 10X magnification. HUVECs in control group formed tube-like structure, which were defined as endothelial cord formations that connected at both ends. The anti-angiogenic activities were accessed by manual counting of the branch points in which at least three tubes joined and total number of tubes using ImageJ software (National Institutes of Health, USA). The average numbers of branches and tubes were calculated from at least 6 randomly photographed fields. Three independent experiments were performed in duplicates for each condition.

3.12 Wound Healing assay

The *in vitro* wound healing assay was performed to access cell migration. Confluent HUVEC monolayers were grown on 6 well plates (SARSTEDT AG & Co, Nümbrecht Germany). The monolayer cells were wounded by scratching with 200µl pipette tip and then washed with warm PBS to remove the non-adherent cells. M200 complete media together with 0.1% DMSO as a control or FKB 1ug/mL, 2.5ug/mL and 5.0ug/mL was added to the wells. The

experiment was performed in duplicates for each condition. After 24h treatment, at least three images of the wound closure were captured using a stereomicroscope (SMZ 1500 Nikon) at 5X magnification. The width of the wound from each photograph was measured using ImageJ software (National Institutes of Health, USA). The initial wound width was considered the same for all conditions and the degree of wound regeneration was calculated as the percentage of the remaining cell free area compared to the vehicle control. Two independently experiments were executed in duplicates for each condition tested.

3.13 Zebrafish strain and drug treatment

The zebrafish angiogenesis model represents a promising alternative in cancer research for the development of antineoplastic and antiangiogenic therapies (Cho *et al.*, 2009; Serbedzija *et al*., 1999). It possesses a complex circulatory system similar to other mammals and provides many advantages compared to other vertebrate angiogenesis model systems, such as ease of experimentation, drug administration and the ability to survive for 3-4 days without functioning circulation (Nicoli & Presta, 2007).

The vascular plan of developing zebrafish embryo starts at 13-somite stage, approximately 13 hour post fertilization (hpf), when endothelial cell precursors migrating from the lateral mesoderm originate the zebrafish vasculature and by 24 hpf a simple circulatory loop consists of the dorsal aorta and axial vein. Angiogenic process continues the blood vessel development and at 48 hpf, subintestinal veins (SIVs) begin to originate from the duct of Curvier. At 72 hpf SIVs will form a vascular plexus across most of the dorsal-lateral aspect of the yolk ball (Serbedzija *et al.,* 1999; Nicoli & Presta, 2007) (Figure 7).

Zebrafish (Danio rerio) embryos were generated by natural pair-wise mating of wild type zebrafish, as described by Kimmel *et al.* (1995). For each mating 4-5 pairs were set up and, on average 100 embryos per pair were generated. Embryos were collected after natural spawning and maintained in E2 medium (EM) (15 mM NaCl, 0.5 mM KCl, 0.49 mM $MgSO_4.7H_2O$, 0.15 mM KH_2PO_4, 0.042 mM Na_2PO_4, 0.1 mM $CaCl_2$ e 0.07 mM $NaHCO_3$, pH 7.2) at 28^{o} C on a 14h light / 10h dark incubator during the whole experiment. The experimental procedures were approved by the Ethic Committee of the Universidade Federal de Minas Gerais (CEUA/UFMG), protocol number 9/2012.

At 48 hours post fertilization (hpf), healthy embryos were manually dechorionated by forceps and placed in 24-well plates (SARSTEDT AG & Co, Nümbrecht Germany) with the drug dissolved in EM at working concentrations. At this stage, zebrafish embryos do not present sub intestinal vessels. In order to prevent toxicity caused by high concentrations of excreted ammonia, only five embryos were kept in each well filled with 1ml of either vehicle or drug solution. Fresh medium containing the drug of interest or vehicle were replaced every 24h, until 72 hpf, when the fish were fixed to further analysis. FKB (LKT Laboratories, Inc), dissolved in DMSO, was kept in -80^{o} C and only thaw and diluted in EM just prior to administration, in order to prevent degradation. Zebrafish larvae are tolerant to DMSO in low concentrations (Hallare *et al*., 2006).

The zebrafish angiogenesis assay was performed as previously described by Serbedzija *et al.* (1999) and is represented in Figure 7.

Embryos were visually inspected for viability, morphological defects and altered behavior. On day 3 of development, embryos were fixed in 4% paraformaldehyde for 2h at room temperature and stained for endogenous alkaline phosphatase activity. Embryos were

then washed twice in phosphate buffered saline with 0.1% tween 20 (PBT) and dehydrated by immersing in 25, 50, 75 and 100% methanol in PBT. Afterwards embryos were rehydrated stepwise to 100% PBT. Before staining, embryos were equilibrated in NTMT buffer (0.1M Tris-HCl pH9.5; 50mM $MgCl_2$; 0.1M NaCl; 0.1%tween 20) at room temperature. After being equilibrated in NTMT for 30 minutes, embryos were stained with 0.34mg/mL nitroblue tetrazolium (NBT) and 0.15mg/mL 5-Bromo-4-chloro-3-indolyl phosphate disodium salt (BCIP) for 10-20minutes in room temperature. Staining reaction was stopped by adding PBT. To remove endogenous melanin in the pigment cells and allow better visualization of the stained vessels, larvae were immersed in a 5% formamide and 10% hydrogen peroxide in PBT for 20 minutes. The embryos were kept in glycerol 80% for about one week and then images were taken at 10X magnification using a stereomicroscope (SMZ 1500 Nikon).

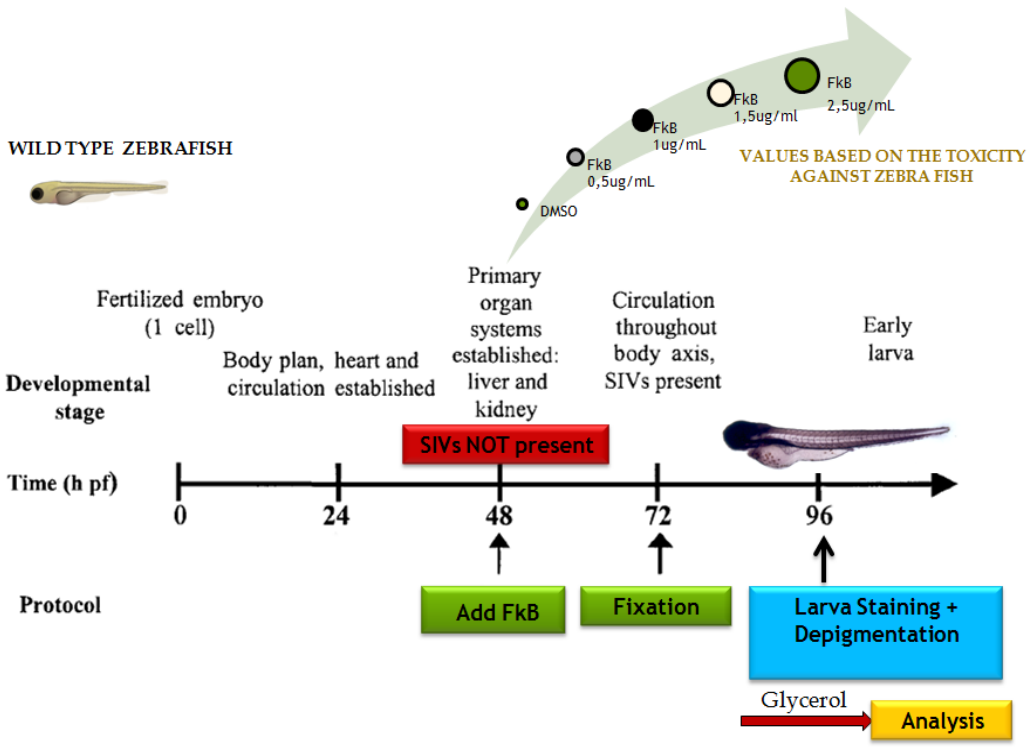

Figure 7: Zebrafish development and angiogenesis assay scheme
Modified from Serbedzija *et al*., 1999.

3.14 Statistical analysis

All data are presented as mean ± SD. Statistical analysis and graphical representation of the data were performed using GraphPad Prism 6.0 (GraphPad Software, San Diego, CA) or OriginLab® software (Corporation, Northampton, MA, USA). Differences between groups were examined using Student's t-test when two groups where compared or oneway analysis of variance (ANOVA) when compared in three or more columns. Two-tailed tests were used for all the hypothesis tests in the present study. Differences were considered statistically significant when $p < 0.05$.

4 RESULTS

4.1 Flavokawain B causes strong antiproliferative effect on ovarian cancer cells in a dose and time response manner

To access the antiproliferative effect of flavokawain B over OVCAR-3 cells the MTT assay was conducted. Cells were treated with increasing concentrations of FKB as indicated or 0.1% DMSO vehicle control for 24 and 48 hours. Results are expressed as the percentage of cell viability relative to control (Figures 8 and 9).

The graphic on Figure 8-A shows that Flavokawain B significantly inhibited the proliferation of OVCAR-3 cells in a dose-dependent manner. The cell viability of OVCAR-3 cells at the concentrations of 7.5; 10; 12.5 and 20µg/mL FKB, was estimated to be respectively 51.88 ± 3.29%; 31.27 ± 3.93%; 19.42 ± 3.60% and 5.81 ± 1.53%. The IC_{50} of FKB towards OVCAR-3 cells was calculate by nonlinear regression of a dose-response curve and estimated to be 7.5±0.30µg/mL (26.38 µM) after 24 h treatment.

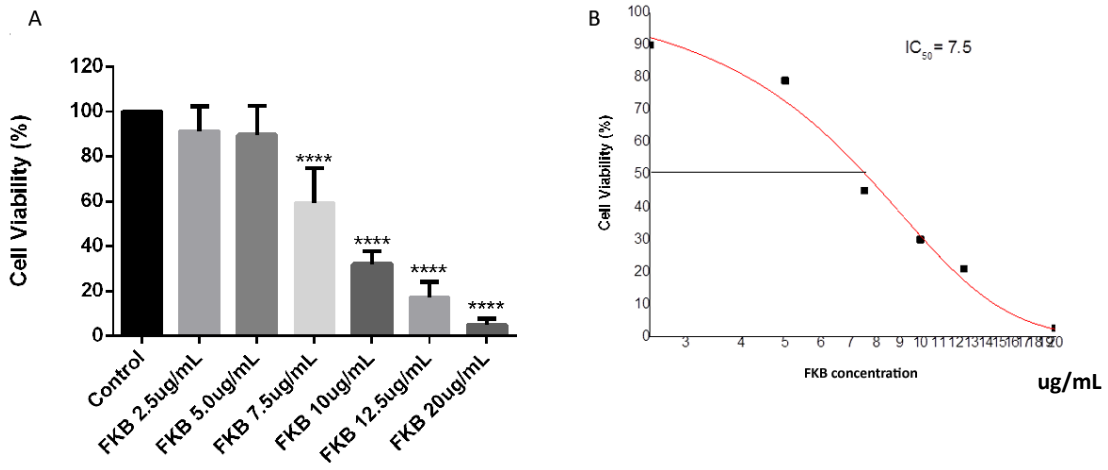

Figure 8: Cell viability of OVCAR-3 cells upon 24h treatment with FKB. A: OVCAR-3 cells were treated with 0.1% DMSO or FKB as indicated. After 24 hours, cell viability was measured by MTT. **B:** FKB IC_{50} was determined by nonlinear regression of the dose-response curve utilizing Originlab® software. Three independent experiments in triplicates were performed. Data are represented as mean ± SD, *p<0.05; **p<0.01; ****p<0.0001. Significance was tested by one-way ANOVA test.

In order to investigate if a longer exposition to FKB could potentiate its action, we have analyzed OVCAR-3 cell viability after 48 hours of treatment. Our results have shown a significant decrease on cell viability at the concentrations of 5.0; 7.5 and 10µg/mL, calculated to be respectively 69.85 ± 6.82; 26.30 ± 4.92 and 23.33 ± 5.40 (Figure 9-A).

FKB also reached a lower IC_{50} after 48h of treatment, estimated to be 5.8±0.90µg/mL (20µM) (Figure 9-B). These results confirm that the FKB antiproliferative action is also time-dependent.

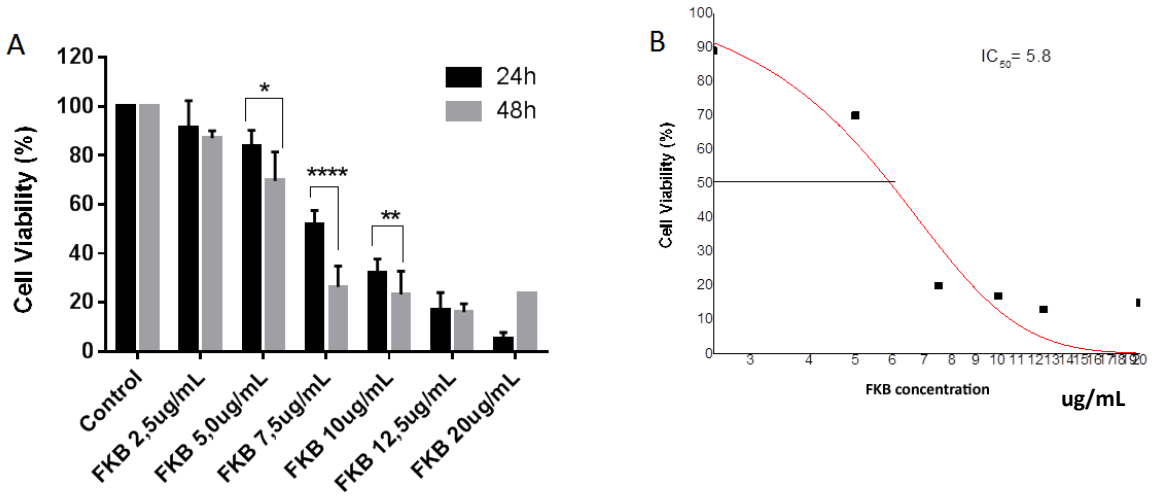

Figure 9: Cell viability of OVCAR-3 cells upon 48h treatment with FKB. A: MTT assay was performed to access OVCAR-3 cells viability after 48h of treatment with FKB or vehicle control as indicated. The results were compared to 24h of treatment. **B:** IC_{50} after 48h treatment with FKB was determined by nonlinear regression of the dose-response curve utilizing OriginLab® software. Columns are representative of three independent experiments; each condition was performed in triplicates. Data are represented as mean ± SD, *p<0.05; **p<0.01; ****p<0.0001. Significance was tested by one-way ANOVA test.

4.2 Flavokawain B induces apoptosis of OVCAR-3 cells

To determine whether the growth inhibitory effect of FKB is through the induction of apoptosis we examined the morphology of control- and FKB-treated cells under light and fluorescence microscopes.

Figures 10 and 11 show typical apoptotic morphologies of FKB-treated cells beginning at the concentration of 5µg/mL, including: cell shrinkage, rounding up, cell membrane blebbing, as well as nuclear condensation.

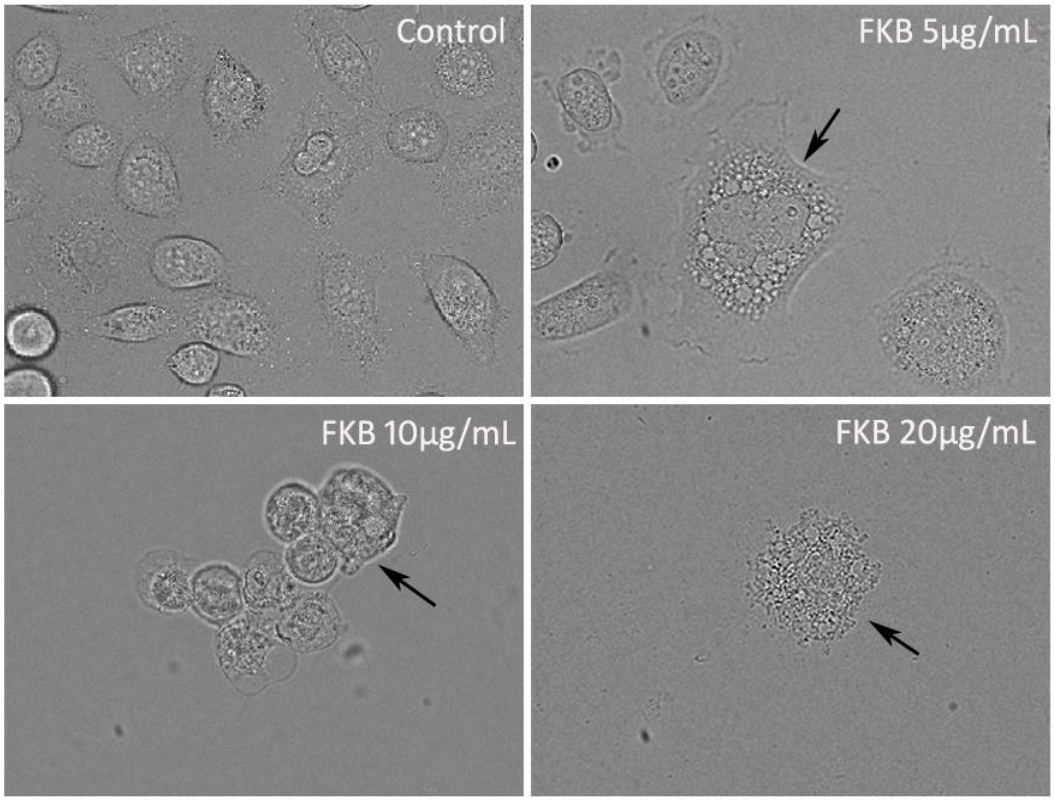

Figure 10: Light microscopy of OVCAR-3 cells treated with FKB. OVCAR-3 cells were grown in coverslips and treated with FKB at the concentrations indicated. DMSO 0.1% was added to the control group. Photographs of three randomly fields were taken at 40X magnification and the representative images of each condition are demonstrated. Arrows indicate typical apoptotic cell morphologies, beginning at the concentration of 5µg/mL, such as cell shrinkage, membrane blebbing and rounding up.

After DAPI and PI staining (Figure 11), different fields were evaluated with the identification of DAPI stained cells with normal nuclei (healthy cells), DAPI stained cells with chromatin condensation (apoptotic cells), as well as, DAPI and PI double stained cells (dead cells). Healthy cells were identified at the control and FKB 5.0µg/mL groups. Cells started to show nuclear condensation at 5.0µg/mL of FKB and at the concentrations of 10 and 20µg/mL FKB, almost all cells were dead under late apoptotic or necrotic mechanisms (double stained cells).

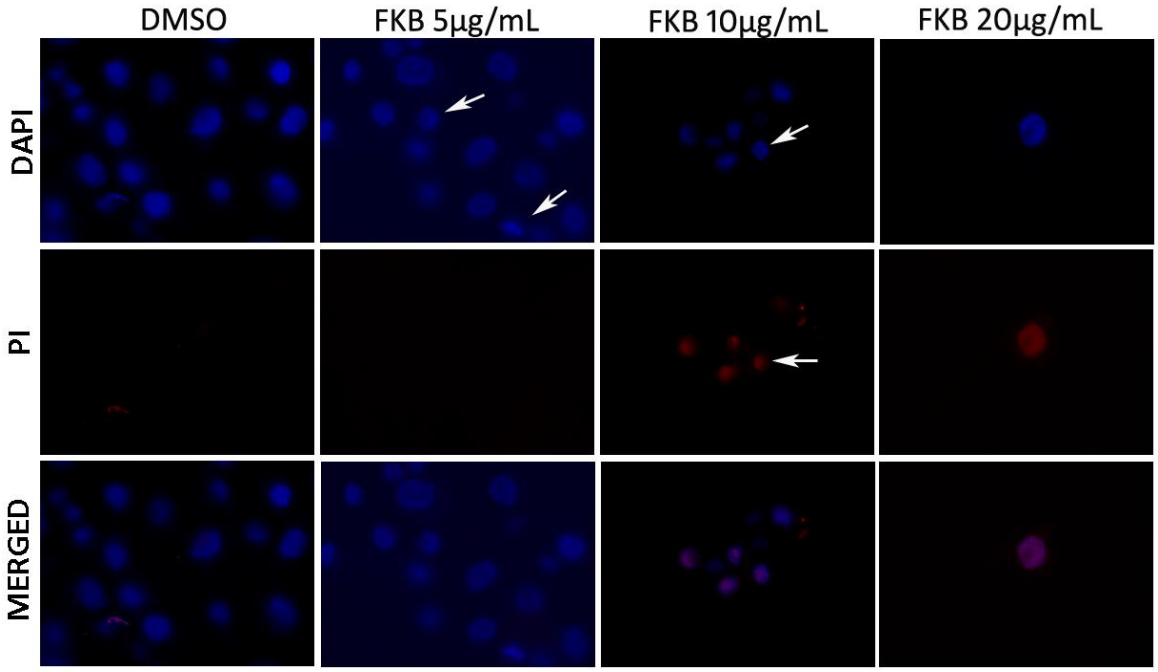

Figure 11: DAPI and PI double staining of OVCAR-3 cells treated with FKB. OVCAR-3 cells were grown in coverslips and treated with FKB at the concentrations indicated. DMSO 0.1% was added to the control group. Double staining with DAPI and PI was executed and images of three randomly fields were taken at 40X magnification. Representative photographs of each condition are demonstrated. Arrows indicate typical apoptotic condensation of nuclei chromatin and DNA fragmentation. Double staining with DAPI and PI indicate dead cells under late apoptosis or necrotic process.

The apoptotic effect of FKB towards OVCAR-3 cells was further evaluated by flow cytometry after Annexin V and -aminoactinomycin D (7-AAD) staining. The detection of

phosphatidylserine externalization is achieved thought Annexin V staining and represents cells under early apoptotic process. Figure 12 shows that with increasing concentrations of FKB, there is a migration of cells from early apoptosis (Annevin V+/7AAD- cells) to late apoptosis/necrosis process (Annexin V+/7AAD+ cells). At the concentration of 5ug/mL there are cells under early (10.7%) and late apoptosis (9.62%). Moreover, FKB 10ug/mL treatment increased the number of dead cells to about 36.8% under late apoptosis and at 20ug/mL almost all cells (85.8%) were dead with cell membrane disruption (7-AAD staining). These results suggest that the inhibitory effect on cell growth might be through induction of apoptosis and, probably, necrosis at higher concentrations.

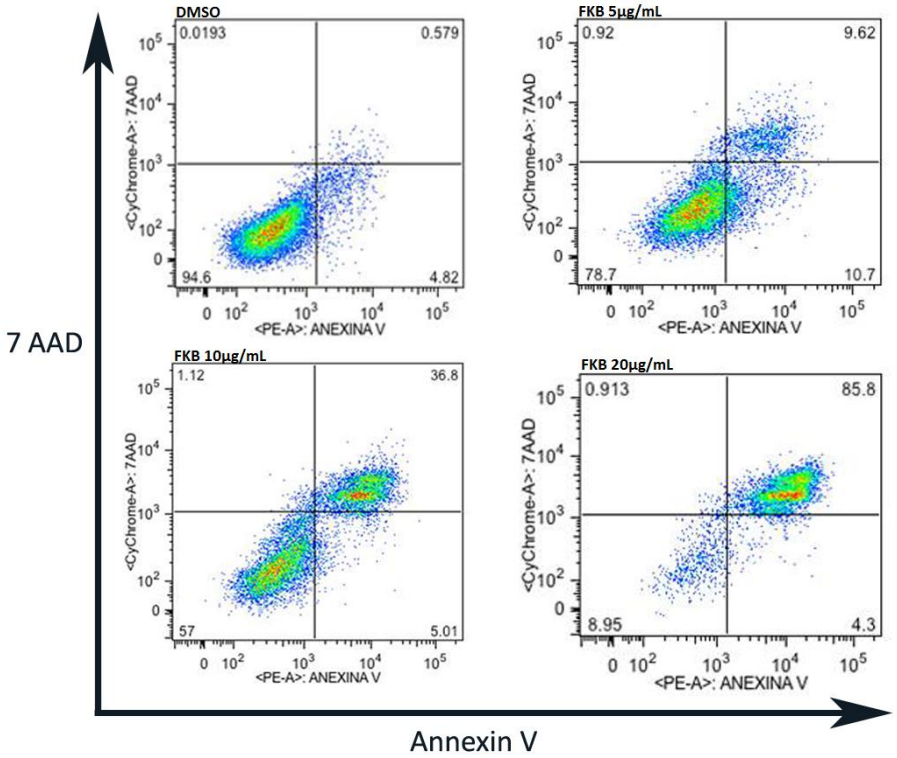

Figure 12: Annexin V and 7 AAD staining of OVCAR-3 cells treated with FKB. OVCAR-3 cells were treated with FKB 5, 10 and 20µg/mL for 24 hours. DMSO 0.1% was used as a control. Cells were stained with Annexin V and 7-AAD and analyzed by flow cytometry. The graphics depict cells under early apoptosis (Annexin V + / PI -) or late apoptosis and necrosis (Annexin V+ / PI +). The results are expressed as percentage of total cells. The experiment was performed in triplicates.

4.3 Flavokawain B is less cytotoxic towards normal cells than to cancer cells

Other publications have demonstrated that FKB has a more potent cytocidal effect against cancer cells than to normal cells. To access this specificity of FKB action, a primary culture of human fibroblasts was established and treated with increasing concentrations of FKB for 24 hours (Figure 13-A). Figure 13-B shows that cell viability reduction was significantly higher in OVCAR-3 cells compared to fibroblasts treated with FKB for 24 hours at the concentrations of 7.5, 10, 12.5 and 20µg/mL. Moreover, while FKB 12.5ug/mL caused more than 80% of reduction on OVCAR-3 cells viability, there was only around 20% decrease on fibroblasts viability.

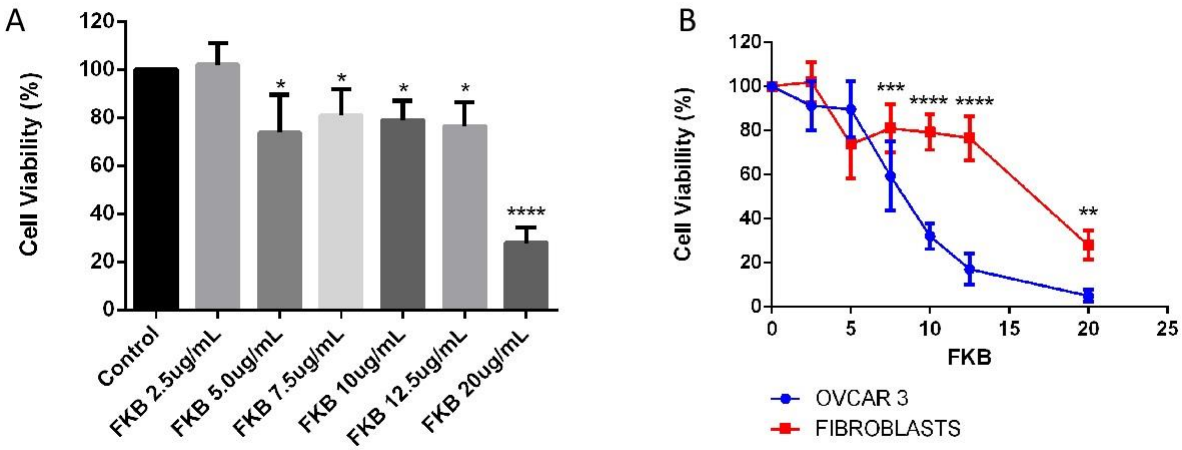

Figure 13: Effects of FKB against normal human fibroblasts cells compared to OVCAR-3.
A: Fibroblasts were seeded in 96-well culture plates. After 24 hours, the medium was changed to fresh medium and treated with 0.1% DMSO alone or FKB (µg/mL) at the indicated doses. After 24 hours of treatment, cell viability was measured by MTT assay. **B:** Dose-response curves comparing the effects of FKB over cell viability in OVCAR-3 and Fibroblasts cells. Results are representative of three independent experiments; each condition was performed in triplicates. Data are represented as mean ± SD, *p<0.05; **p<0.01;***p<0.001; ****p<0.0001. Significance was tested by one-way ANOVA test.

The IC_{50} of FKB against fibroblasts and OVCAR-3 cells were calculated by nonlinear regression and estimated to be respectively, 15ug/mL (52.75uM) and 7.5ug/mL (26.38µM), after 24 hours treatment. The selectivity index of FKB against ovarian cancer cells was calculated based on the ratio of the IC_{50} obtained for normal and cancer cell lines and reveals that FKB was 2.0 times more potent against OVCAR-3 cells (Table 7).

Table 7: The selectivity index of FKB against ovarian cancer cells compared to normal cells

Cell Lines	**Flavokawain B IC_{50} (µg/mL)**
OVCAR-3	7.5±0.30
Fibroblasts	15±2.0
Selectivity index	
Fibroblasts(IC_{50})/OVCAR-3(IC_{50})	~2.0

4.4 Flavokawain B reduces Bcl-2 protein expression and increases de Bax:Bcl-2 ratio in OVCAR-3 cells

It was extensively described in several cancer cell lines that FKB apoptotic effect involves the mitochondrial pathway with cleavage of caspase 9/3. To elucidate if the intrinsic pathway is also involved in the FKB induction of OVCAR-3 cell death we analyzed the expression of Bax, Bcl-2, Bcl-xL, Bak and AIF proteins upon treatment with increasing concentrations of FKB or vehicle control (Figure 14).

The death stimulus that triggers the intrinsic pathway results in increased mitochondrial permeability, loss of mitochondrial transmembrane potential and release of

pro-apoptotic proteins from the intermembrane space to the cytosol, such as cytochrome c and AIF. The control and regulation of these apoptotic mitochondrial events occurs through members of the Bcl-2 family of proteins that can be either pro-apoptotic or anti-apoptotic. Bcl-2 and Bcl-xL are anti-apoptotic proteins, while Bax and Bak are pro-apoptotic proteins. Bax and Bak triggers cytochrome c release, whereas Bcl-2 and Bcl-xL inhibit it.

Compared with vehicle control, treatment of OVCAR-3 cells with FKB reduced Bcl-2 protein expression of about 20% compared to control at 2.5; 5.0 and 7.5μg/mL. This effect was more pronounced at 10μg/mL with around 31% reduction on Bcl-2 level (Figures 14-A and 14-B). The expression of Bcl-xL, however, didn't change upon treatment with FKB (Figures 14-C and 14-D)

Bax gene encodes different active isoforms. The antibody we used could recognize Bax_{α} (21kDa) and Bax_{β} (24kDa) bands. We considered both bands in our estimation of total Bax expression. Figure 14-G shows an increase tendency of total Bax protein, but not statistically significant (Figure 14-H). On the other hand, the corresponding Bax: Bcl-2 protein ratio was significantly unregulated at 10μg/mL of FKB as shown in Figure 15. The expression of Bak and AIF, the other pro-apoptotic proteins investigated, didn't change between the control and treated groups (Figures 14-E, 14-F, 14-I and 14-J), although there was a tendency of increase in AIF expression at higher concentrations of FKB.

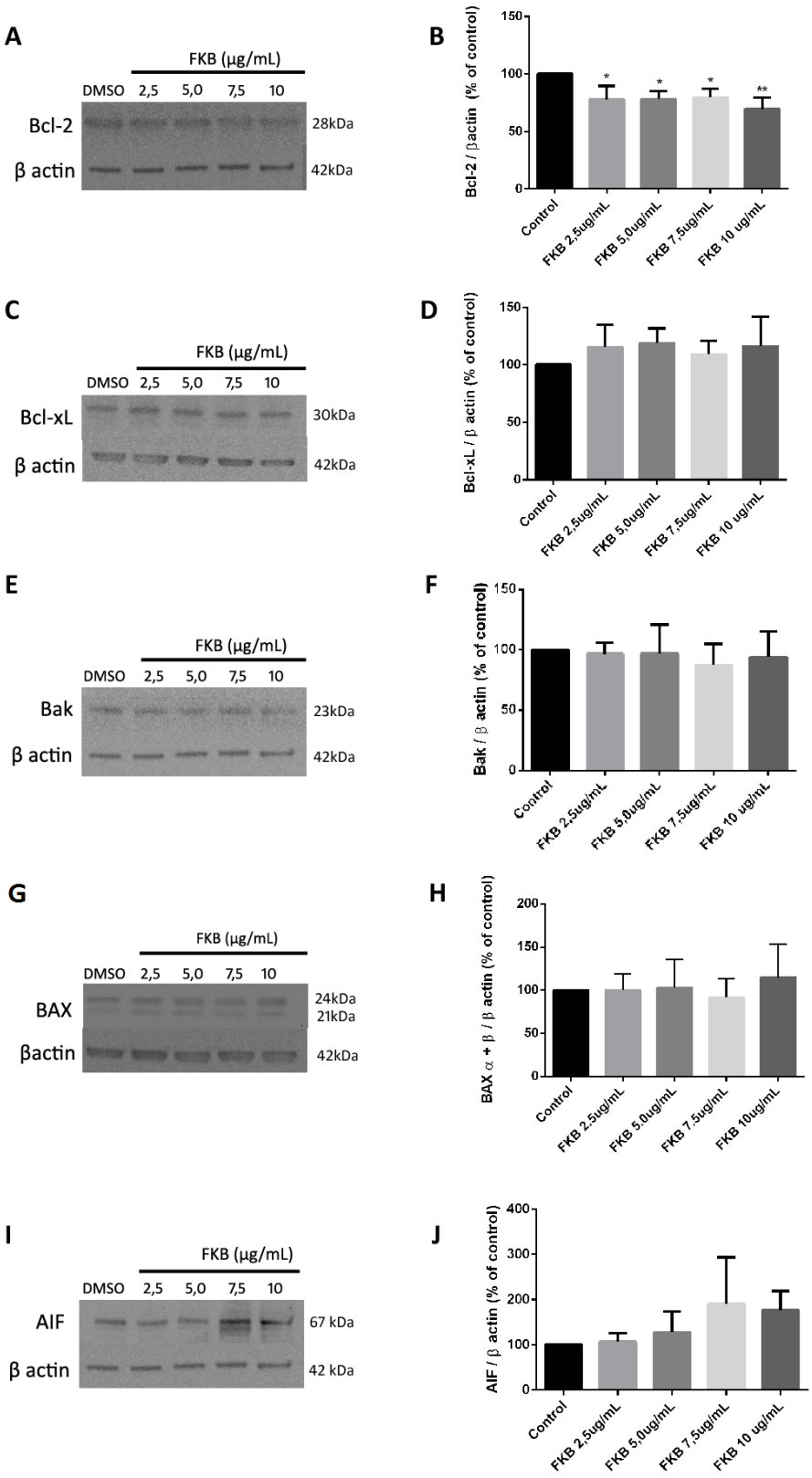

Figure 14: Western-Blotting analysis of apoptotic proteins expression. OVCAR-3 cells were treated with FKB for 24 hours. Cell lysates were separated by SDS-PAGE and analyzed for Bcl-2 (**A,B**), Bcl-xL (**C,D**), Bak (**E,F**), Bax (**G,H**) and AIF (**I,J**) by Western blotting. β-actin was used as a control. One representative image of three experiments is presented. Data are represented as mean ± SD, *p<0.05; **p<0.01. Significance was tested by one-way ANOVA test.

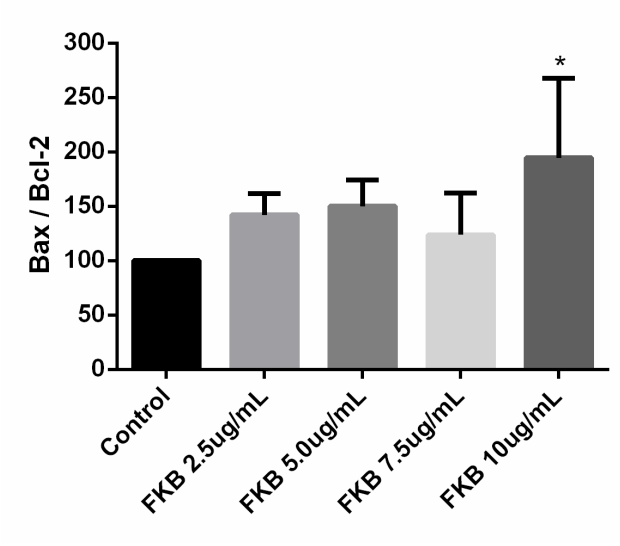

Figure 15: Bax:Bcl-2 ratio of OVCAR-3 cells after 24h treatment with FKB. A commitment to apoptosis was measured by examining any increase in the ratio of Bax (pro-apoptotic protein) expression to Bcl-2 (anti-apoptotic protein) expression. The densitometric analysis of Bax:Bcl-2 ratio was performed in all treatment groups. Data are represented as mean ± SD, *p<0.05. Significance was tested by one-way ANOVA test.

4.5 Flavokawain B inhibits PI3K/Akt pathway activation in OVCAR-3 cells

PI3K-Akt signaling pathway activation occurs frequently in epithelial ovarian cancer patients and its downstream transcription factors affects important biological processes such as cell proliferation, survival, motility, cell-cycle control and angiogenesis. We therefore investigated whether FKB treatment could inhibit the activation of PI3K-Akt pathway by accessing Akt phosphorylation. Our results showed that FKB 24 hour treatment significantly inhibited the activation of Akt in all concentrations tested (2.5; 5.0; 7.5 and 10µg/mL) in a dose-dependent manner (Figure 16). Akt activation was more than 50% reduced at 10µg/mL. Total Akt expression, however, did not significantly change upon treatment with FKB.

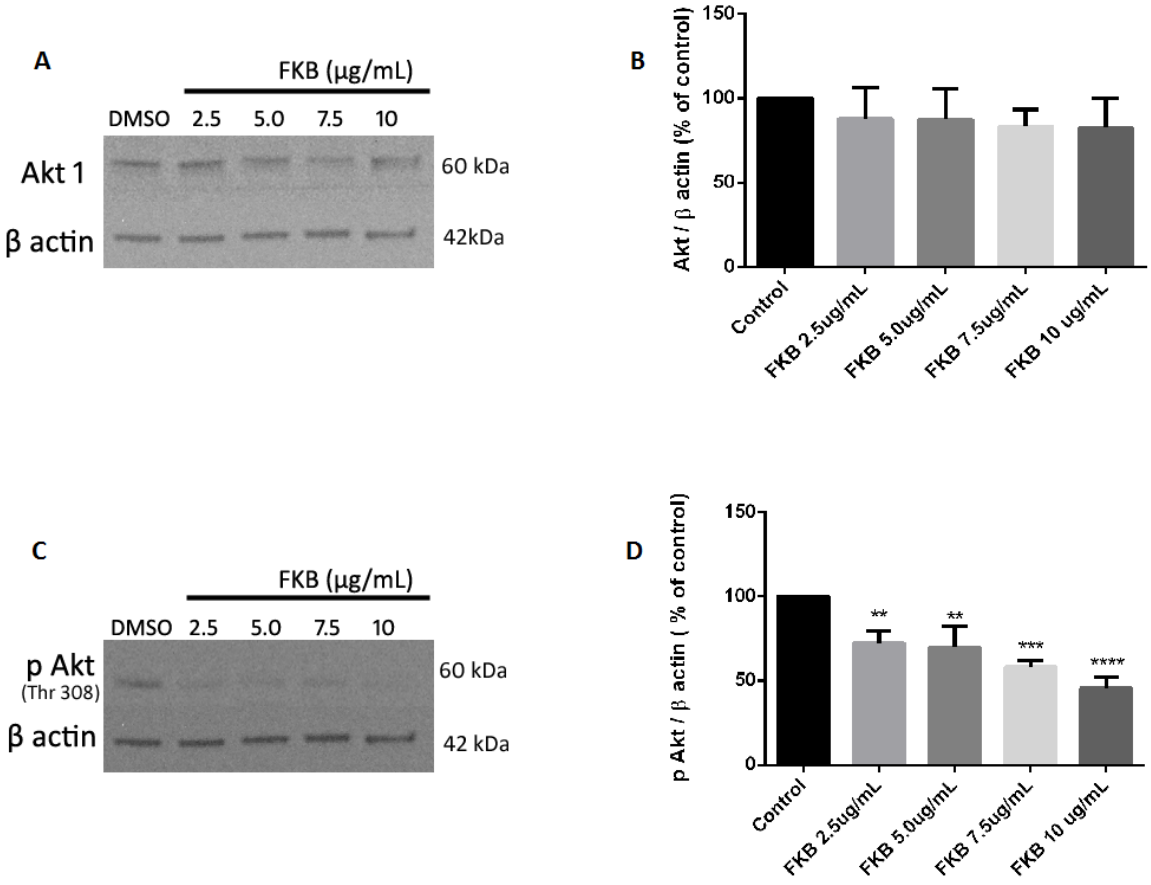

Figure 16: FKB downregulates Akt activation in OVCAR-3 cells. OVCAR-3 cells were treated with DMSO or FKB at the concentrations indicated for 24 hours. Aliquots of cell lysates were separated by SDS-PAGE and analyzed for Akt (**A, B**) and phospo-Akt (**C,D**) by Western blotting. β-actin was used as an internal control to monitor equal loading. One representative image of three experiments is presented. The desitometric analysis of the bands was performed using ImageJ software. Data are represented as mean ± SD, *p<0.05; **p<0.01. Significance was tested by one-way ANOVA test.

4.6 FKB inhibits endothelial cells proliferation, migration and tube formation

Angiogenesis play a major role in tumor growth, progression and metastasis and is thought to be particularly crucial in the persistence of EOC. Considering the importance of angiogenesis in the progression of ovarian cancer and previous reports of the potential antiangiogenic effects of FKB, we initially evaluated the FKB anti-angiogenic potential *in vitro.*

In vitro, endothelial cells can spontaneously form a three-dimentional tubular capillary-like network on Matrigel culture. To observe the influence of FKB on tube formation of HBMEC cells under the stimulus of VEGF 15ng/mL, time lapse microscopy was performed. The concentration of FKB 5µg/mL was utilized, since it did not change HBMEC cells viability according to the MTT assay (Figure 17-B). After 4 hours of experiment we can observe endothelial cells migration and formation of tubes in the control group with 0.1% DMSO, but not in the FKB treated cells as shown in Figure 17-A.

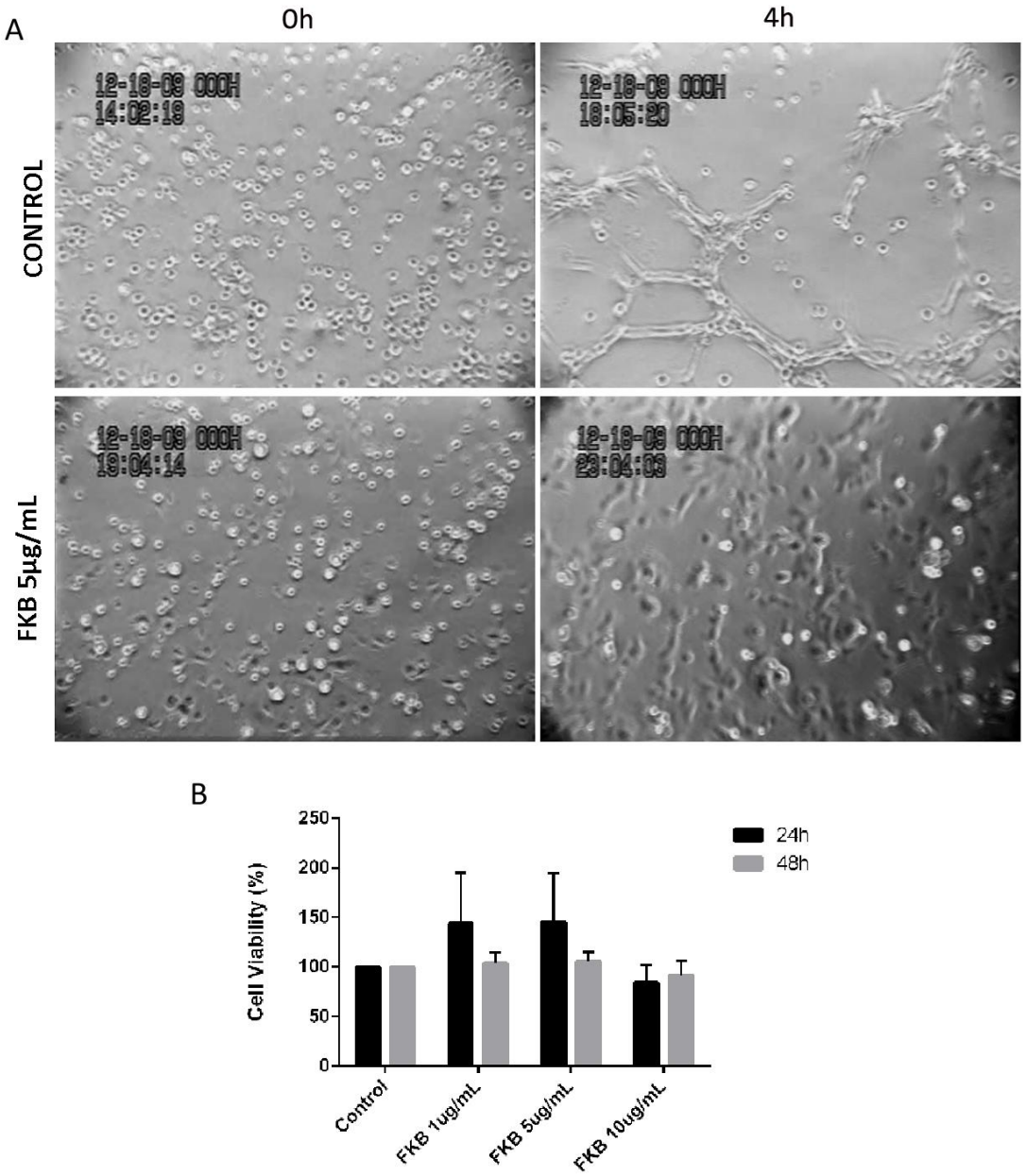

Figure 17: FKB 8h treatment inhibits capillary tube formation of endothelial cells under the stimulus of VEGF . **A:** HBMEC were seeded in a 100mm dish coated with Matrigel® and 15ng/mL of VEGF was added to the cell media. DMSO 0.1% was added to the control dish and 5µg/mL of FKB was added to the treated dish. Cells were placed inside a transparent incubator at 37^0C and 5% CO_2 for 8 hours and time-lapse microscopy was performed using a FV1200 microscope. **B:** HBMEC cells were seeded in 96-well plates and treated with different concentrations of FKB for 24 and 48 hours, as indicated. Cell viability was accessed with MTT assay. FKB did not significantly change HBMEC cell viability in all concentrations tested. Data are represented as mean ± SD. Significance was tested by one-way ANOVA test.

Going further, to confirm our findings, we examined the influence of FKB on HUVEC cells migration and tube formation. First, a survival curve was obtained with the MTT assay, since endothelial cell proliferation is also important and necessary for angiogenesis. Figure 18 shows that FKB 1.0 and 2.5µg/mL did not significantly changed HUVEC cell viability; FKB 5µg/mL caused around 20% of cell death and there was a markedly reduction in cell viability at the concentrations of 7.5µg/mL and 10µg/mL of about 80% and 90% respectively. The other experiments were performed with the concentrations that did not significantly impaired endothelial cells viability in order to confirm the antiangiogenic effects of FKB.

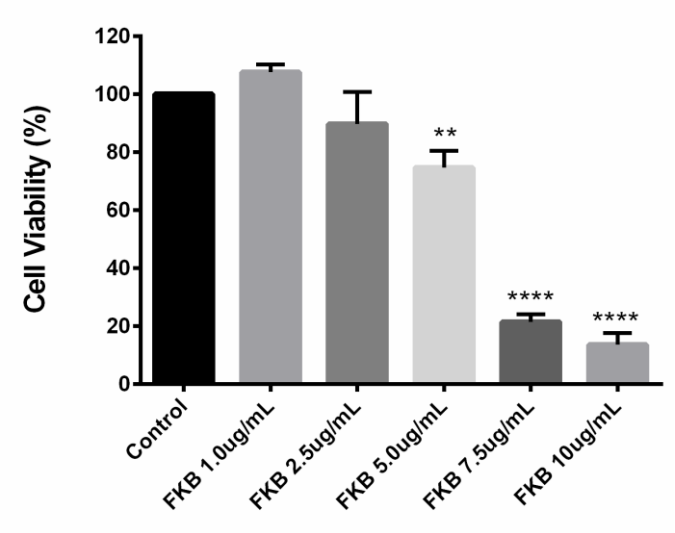

Figure 18: Cell viability of HUVEC cells treated with FKB for 24 hours. HUVEC cells were plated in 96-well culture plates. After 24 hours, the medium was changed to fresh medium and treated with 0.1% DMSO alone or Flavokawain B at the indicated doses. After 24 hours of treatment, cell viability was measured by MTT assay. Columns are representative of three independent experiments; each condition was performed in triplicates. Data are represented as mean ± SD, **p<0.01;***p<0.001; Significance was tested by one-way ANOVA test.

Wound-healing assay was also performed to evaluate endothelial cell migration, which is another essential step for endothelial cells to form new blood vessels. The percentage of cell migration was determined compared to the control group. Figure 19 shows that in the control group the wound was completely closed by migrated cells after 24 hours. In contrast, FKB caused a clear and significant inhibition of HUVECs migration. At the non-toxic concentration of 2.5µg/mL the percentage of migrated cells was just 29.12± 13.74% relative to control.

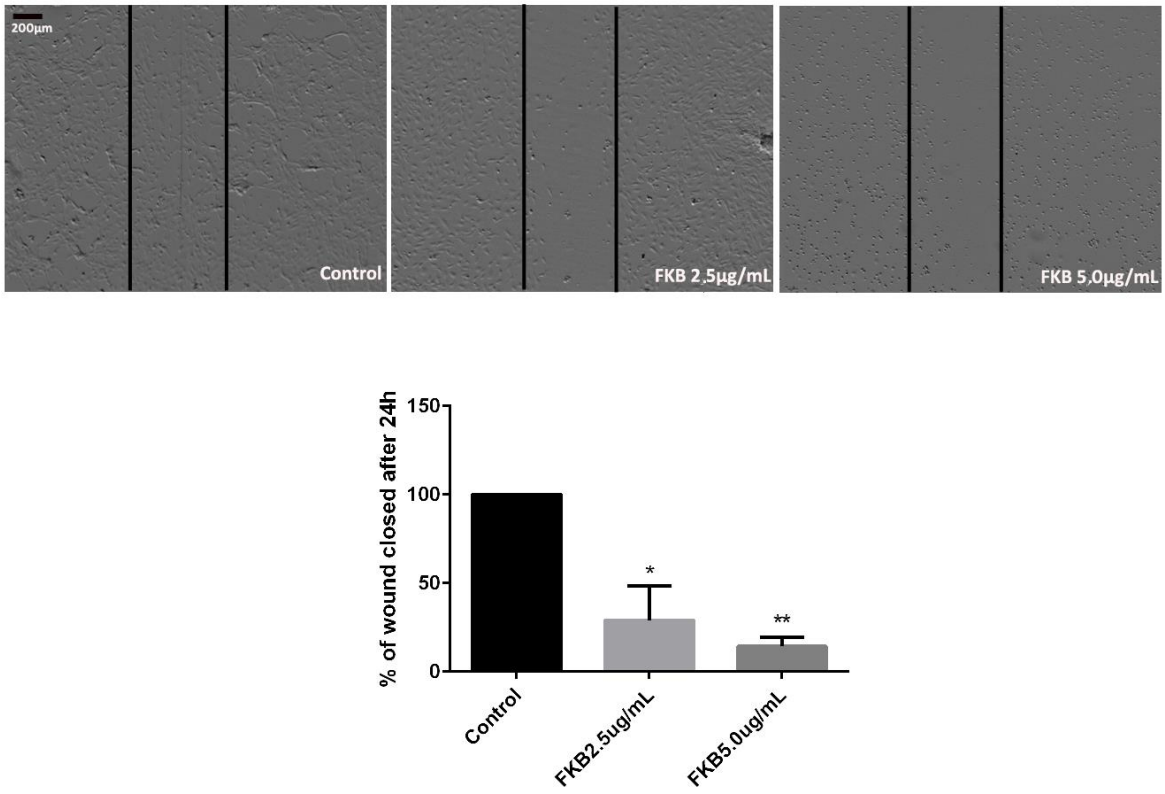

Figure 19: FKB inhibits endothelial cell migration. Confluent monolayers of HUVEC on 6-well plates were wounded with a 200µl pipette and treated with FKB or vehicle for 24 hours. Images of the wound closure were captured using a stereomicroscope (SMZ 1500 Nikon) at 5X magnification. The width of the wounds from each photograph was measured using ImageJ software. The initial wound width was considered the same for all conditions and is represented by the black vertical lines. Total monolayer regeneration was expressed as a percentage of mean wound width of each treatment compared to the vehicle control. Two independent experiments were performed in duplicates for each condition. Data are represented as mean ± SD, *p<0.05; **p<0.01. Significance was tested by one-way ANOVA test.

In addition, tube formation assay was conducted to evaluate the effects of FKB on HUVEC capacity to form capillary tube like structures. As shown in Figure 20, FKB dramatically inhibited HUVEC tube formation in a dose-dependent manner, suggesting that it indeed regulated angiogenesis *in vitro*. The percentage of tube formation in FKB 2.5 and 5.0µg/mL treated groups were respectively, 38.44±3.95% and 25.44±5.69 relative to control, considering branch points number.

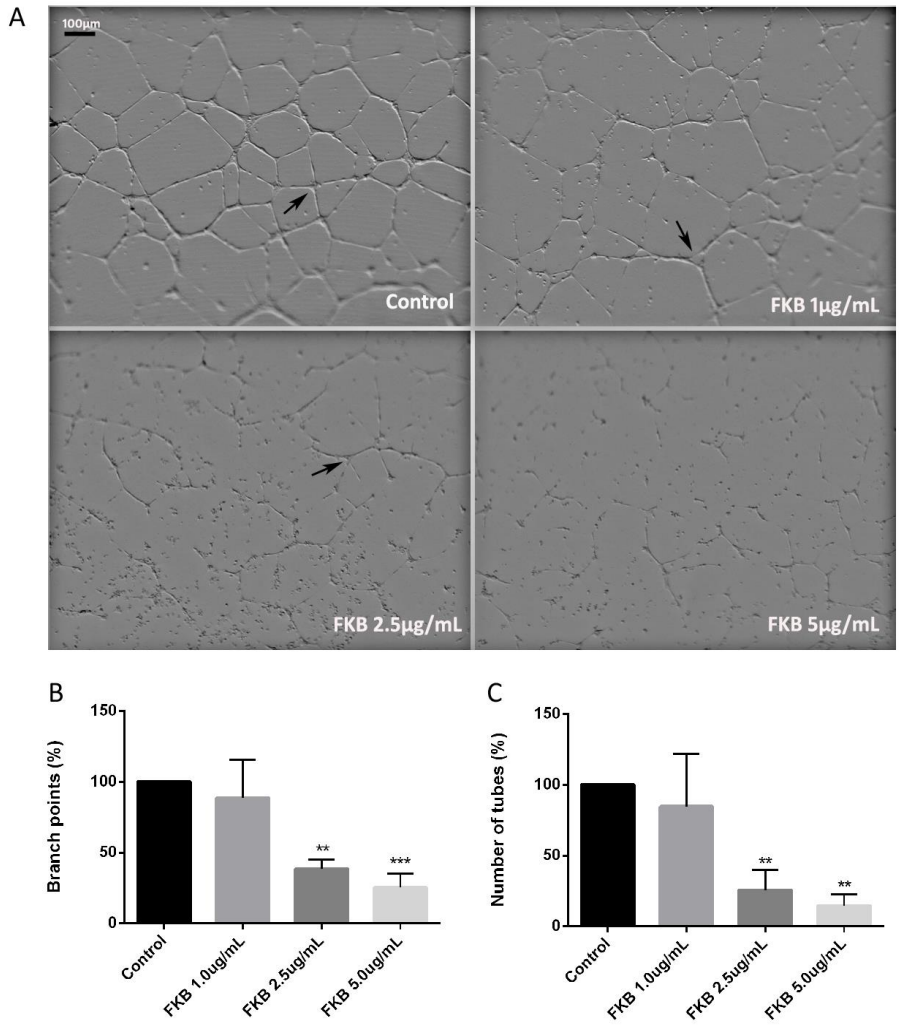

Figure 20: FKB inhibits capillary tube formation in cultured endothelial cells. A: HUVECs were seeded on Geltrex® coated 24-well plates and incubated with FKB and vehicle for 18 hours. At least 6 images were randomly taken from each well. This figure is representative of three experiments performed in duplicates. **B, C:** Branch points (indicated by the arrows) and tube structures were counted to quantify endothelial tube formation. Tube formation was calculated as the percentage of branch points or tubes compared to vehicle control. Data are represented as mean ± SD, **p<0.01. Significance was tested by one-way ANOVA test.

4.7 FKB suppresses angiogenesis in vivo in a Zebrafish model

The zebrafish angiogenesis model represents a promising alternative in cancer research for the development of antineoplastic and antiangiogenic therapies. Endogenous alkaline phosphatase (AP) staining of zebrafish embryos permitted adequate visualization of subintestinal veins (SIVs), which are normally completely formed at 72 hours post fertilization (hpf). Figure 21-A shows a representation of SIV development. Prior to the experiments, 48 hpf and 72 hpf untreated larvae were AP stained to access SIV formation. At 48 hpf SIVs were absent and at 72 hpf SIVs were completely formed with normal characteristic patterns (Figures 21-B).

A dose response toxicity curve was also performed, based on the concentration of FKB utilized in cells (0.5; 1.0; 1.5; 2.5; 5.0 and 10µg/mL). Noteworthy, zebrafish embryos did not show signs of toxicity until the concentration of 5.0µg/mL, which is already toxic and has led to death some embryos within less than 24h of treatment (data not shown). At the concentration of 10µg/mL, the formation of SIVs were absent, however FKB was toxic and pigment alterations was observed in the embryos, as shown in Figure 21-C. Treatment with FKB for 24 hours at concentrations between 0.5 and 2.5µg/mL did not altered morphological or behavior pattern, screened visually (data not shown). Therefore, the non-toxic concentrations 0.5; 1.0; 1.5 and 2.5µg/mL of FKB were used in our next experiments.

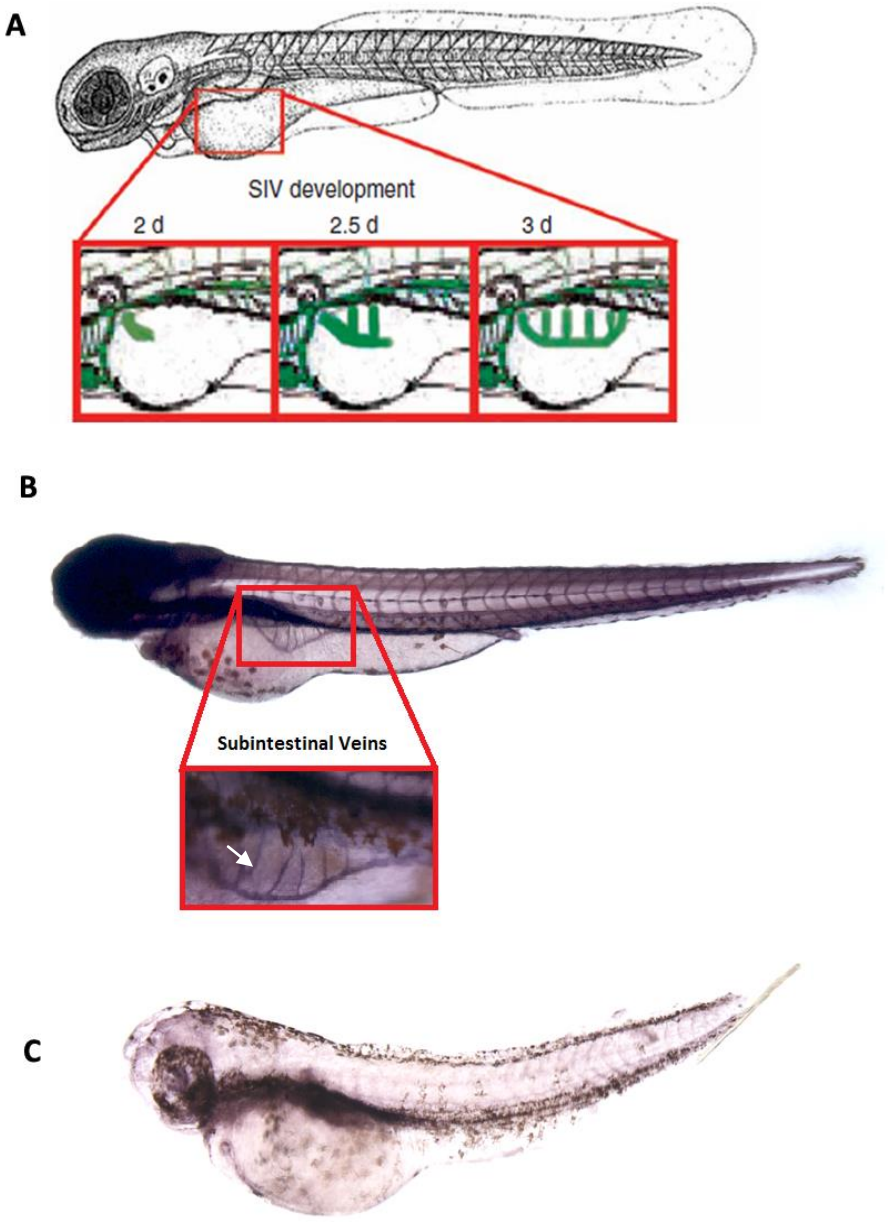

Figure 21: SIV formation and toxic effect of FKB towards zebrafish. **A:** Lateral view scheme of a zebrafish larva, showing the SIV development post fertilization (Extracted from Nicoli & Presta, 2007). **B:** Lateral view scheme at 3X and 10X magnification of normal SIV development in a zebrafish 72 hpf control embryo after alkaline phosphatase staining. The black arrow indicates the intersegmental vessels. **C**: Lateral view at 3X magnification of FKB 10µg/mL 72 hpf treated embryo with completely inhibited SIV formation and significantly altered pigmentation.

The angiogenesis rate was quantified by manual counting of the SIVs intersegmental vessels observed on the left and right sides of the embryo. Figure 22 shows the representative results of two replicated experiments.

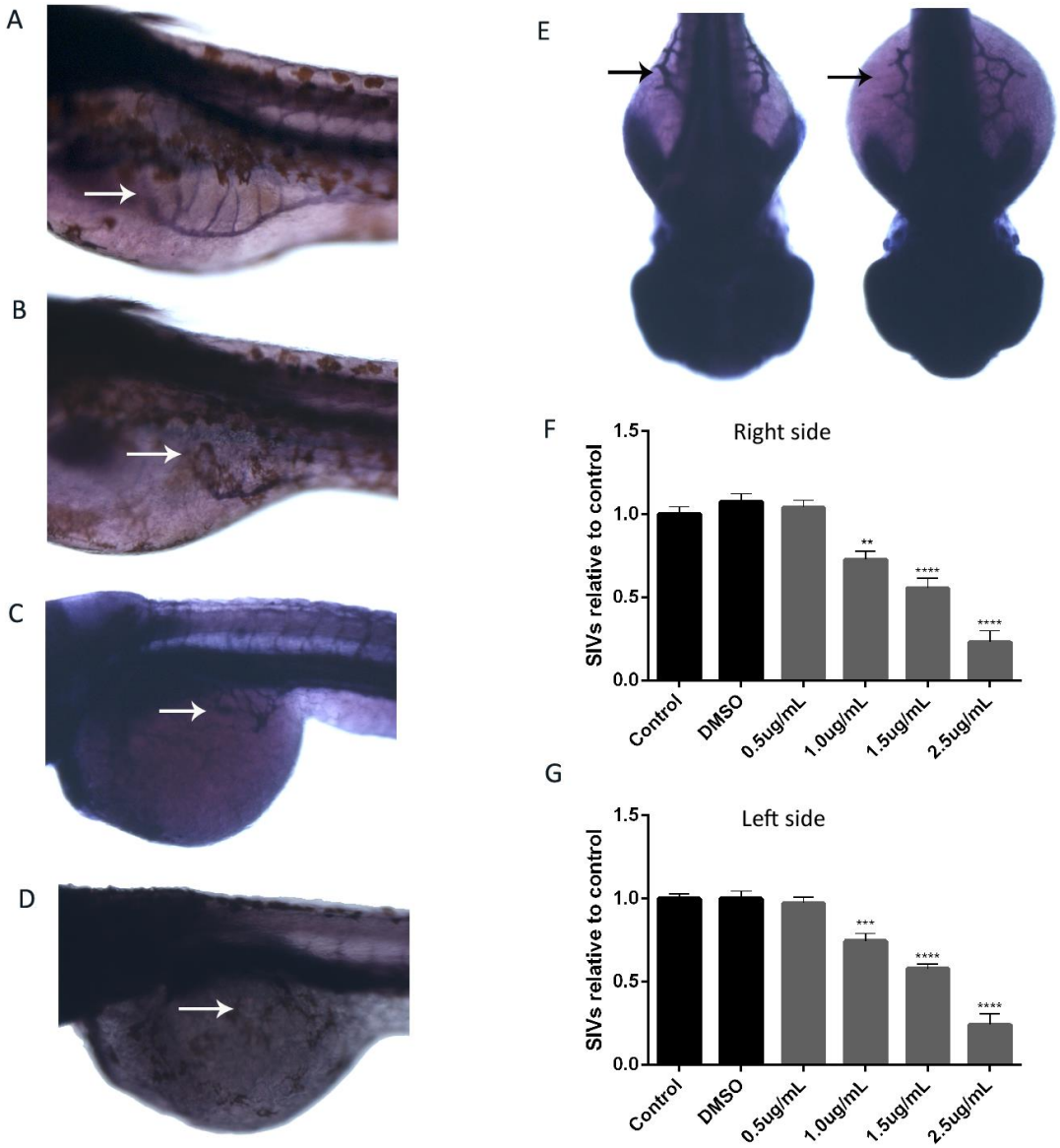

Figure 22: FKB blocks angiogenesis process in Zebrafish. Lateral view (**A,B,C,D**) and dorsal view (**E, F**) at 10X magnification of AP stained embryos at 72 hpf. SIVs locations are indicated by the white arrows. Embryos were treated with FKB or vehicle control for 24 h. **A:** 0.1% DMSO had no effect on vessel formation. **B:** FKB 1µg/mL caused reduction of SIV intersegmental vessels. **C:** FKB 1.5µg/mL caused reduction and distortion of SIV. **D:** FKB 2.5µg/mL completely blocked SIV formation. **E:** Dorsal view of control larva. **F:** Dorsal view of FKB 1.5µg/mL treated embryo with distorted SIV formation. **G, H:** Intersegmental vessels in the right and left sides of the embryos were manual counted. Images are representative of two experiments independently done (n=10 per group). Data are represented as mean ± SD.** p<0.01; ***p<0.001; ****p<0.0001. Significance was tested by one-way ANOVA test.

The exposure of the embryos to FKB for 24 hours showed a dramatic reduction of SIV in a dose-dependent manner. At a concentrations of 1.0; 1.5 and 2.5µg/mL of FKB, SIV formation relative to control was respectively, 74.36 ± 4.47% 57.84 ± 2.90% and 23.96 ± 6.62% on left side and 72.59 ± 4.92% ; 55.55 ± 5.73% and 22.96 ± 6.89% on right side. A complete inhibition of SIV formation was observed in some 2.5µg/mL FKB treated embryos (Figure 22-D). These findings suggest that FKB might be an effective antiangiogenic drug, since it could reach maximal effective action at a concentration with no toxic signs in the zebrafish angiogenesis model.

To determine if FKB had any intervention on zebra fish embryo development, the embryos body length were measured, according to Parichy *et al.,* 2009, before treatment at 48 hpf and after treatment at 72 hpf (Figure 23). The 72 hpf FKB exposed larvae length was compared to the 72 hpf controls and a reduction was observed on larva growth at the concentrations of 1.5 and 2.5µg/mL FKB. However, the 72 hpf larvae of these two FKB treated groups when compared to the 48 hpf larvae, have a significantly bigger length. These findings suggest that the decrease on larva growth noticed after FKB treatment might be due to vascular impairment and not because of postponed maturation of the embryos, since they continue to grow even in the presence of FKB.

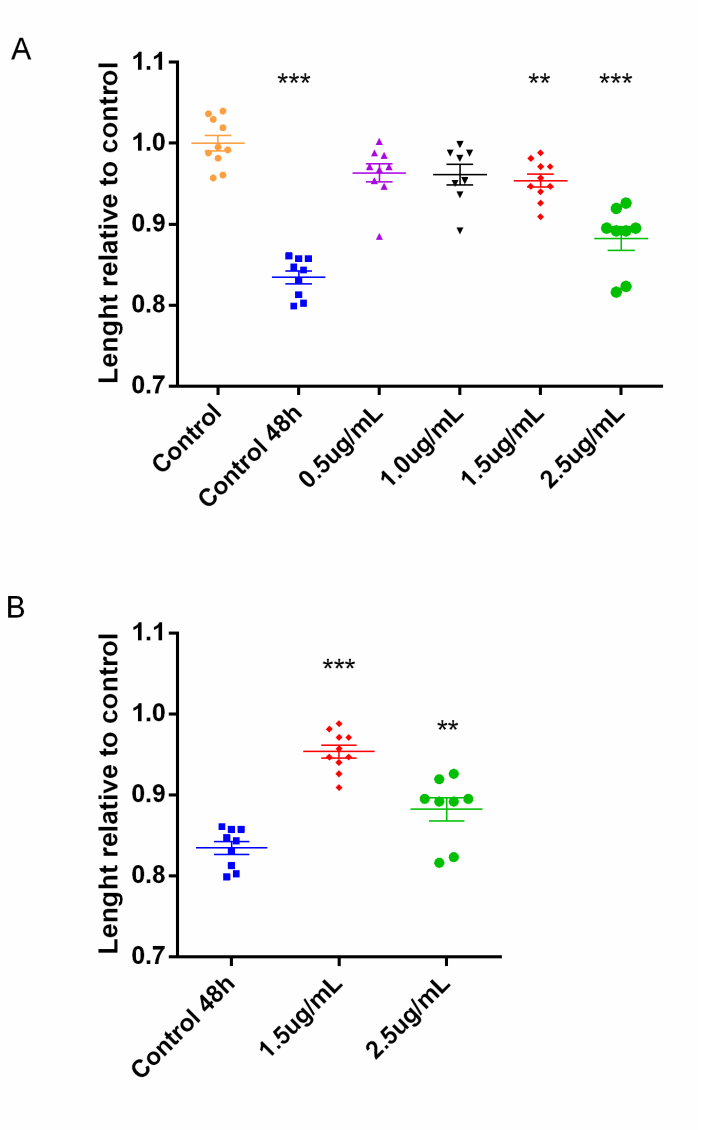

Figure 23: FKB does not impair embryos maturation or development. Larvae length was measured at 48 hpf, before treatment, and at 72 hpf, after treatment with vehicle control or FKB 0.5; 1.0; 1.5 and 2.5µg/mL. **A:** The larvae length of each group was measured and compared to the control 72 hpf. **B:** Length of controls at 48 hpf were compared to FKB 1.5 and 2.5µg/mL treated groups. Data are represented as mean ± SD, (n=9 per group), **p<0.01;***p<0.001; ****p<0.0001. Significance was tested by one-way ANOVA test.

5 DISCUSSION

Natural products have shown promising anti-cancer activity. Chalcones are precursor compounds for flavonoids synthesis in plants and have been described as potential therapeutic agents against cancer cells, by provoking apoptosis, inhibiting cellular proliferation, invasion and angiogenesis (Mahapatra *et al*., 2015). Flavokawain B is a chalcone encountered in Kava-kava root extract, which is traditionally used in South Pacific islands in the form of a drink (Singh, 1992). Epidemiological data showing less incidence of cancer in these regions encouraged many researches to seek for a dietary chemopreventive source that culminated with the association of Kava with anticancer properties (Steiner, 2000).

Many studies have identified flavokawain B as the most potent anti-cancer and anti-inflammatory compound of Kava extract. It has demonstrated impressive cytocidal action against prostate, uterine, lung, breast, oral, synovial and bone cancer cells, mainly through apoptotic mechanisms (Zi & Simoneau, 2005; Li *et al*., 2008; Kuo *et al.*, 2010; Tang *et al.*, 2010; Zhou *et al.*, 2010; An *et al.*, 2012; Eskander *et al.*, 2012; Hseu *et al.*, 2012; Li *et al.,* 2012; Lin *et al.*, 2012; Sakai *et al.*, 2012; Ji *et al.*, 2013; Kwon *et al.*, 2013; Abu *et al.*,2014, Abu *et al*., 2015). Apoptosis is a programmed form of cell death characterized by several cell morphological features. There are two main apoptotic pathways: the extrinsic or death receptor pathway and the intrinsic or mitochondrial pathway. Both cascades converge to the activation of caspases that have proteolytic activity, leading to cell death (Elmore, 2007). The ability of cancer cells to expand and proliferate is directly related to their capacity to evade from programmed cell death, which is considered one of the great hallmarks of cancer (Hanahan & Weinberg, 2011). Therefore, one of the targets in cancer therapy is to induce tumor cells death by restoring the apoptotic machinery.

Epithelial ovarian carcinoma is the leading cause of death among patients with gynecologic cancers. Current management of ovarian cancer is radical surgery and chemotherapy, which are directed at established cancers, not at the mechanisms by which cells become neoplastic (Kurman & Shih, 2016). Despite these multiple modalities of treatment, recurrence and the development of resistance to chemotherapy are common, patients continue to have one of the lowest 5-year survival rates and cure remains elusive (Kim *et al.*, 2012). Hence, the development of new effective therapeutic agents against ovarian cancer, targeting its specific molecular pathways is urgently needed to improve patient survival.

In our study we identify, for the first time, FKB as a promising strategy in the treatment of ovarian cancer, by the reduction of ovarian cancer cells proliferation and induction of cell death. The OVCAR-3, human ovary epithelial adenocarcinoma cell line was utilized in our studies. It has been established from the malignant ascites of a patient with progressive disease, resistant to chemotherapy. Thus, it is considered a good cell model for the discovery of new adjuvant agents against chemo-resistant ovarian malignancies (Hamilton *et al*., 1983; Sociale *et al*.,2016).

In the present study, MTT assay was utilized to determine the cytocidal action of FKB against ovarian cancer cells by the evaluation of cell viability. It is one of the most commonly used assays for the *in vitro* screening of new potential bioactive agents against cancer (Denizot & Lang *et al.*, 1986; Vistica *et al*., 1991). Our results have demonstrated that upon treatment with FKB, OVCAR-3 cells had a significant reduction on cell viability in a time and dose dependent manner. Comparing the IC_{50} of FKB towards ovarian cancer cells to other

cancer cells already tested in the literature and considering similar conditions, we notice that FKB was more potent against bladder, colon, prostate androgen receptor (AR) negative and melanoma cancer cells than to OVCAR-3 cells. On the other hand, OVCAR-3 cells were more sensitive to FKB than oral epidermal carcinoma, breast cancer, carcinoma of the cervix, lung adenocarcinoma and prostate cancers AR positive. However, this is just a simplistic analyzes, since cell viability results and the IC_{50} values can be strongly influenced by variations between studies, such as cell culture conditions, drug handling and storage, MTT assay protocol and the range of drug concentrations tested to determine drug-response curves (Hatzis *et al.,* 2014).

To elucidate the possible mechanisms involved on cell death induction by FKB, we analyzed cell morphology after exposure to increasing concentrations of the chalcone. Similar to the observations described in other studies with different cancer cell lines, OVCAR-3 cells showed typical apoptotic morphologies, including cell shrinkage, bleebing, rounding up and pyknosis, suggesting that apoptosis was triggered by FKB (Tang *et al.*, 2010; Eskander *et al.*, 2012; Ji *et al*., 2013).

Flow cytometry analysis with Annexin V and 7AAD staining has been used to better elucidate if cells were dying through apoptotic or necrotic mechanisms. The externalization of phosphatidylserine to the outer cell plasma membrane is one of the markers to phagocytic recognition of apoptotic cells. Annexin V is a recombinant phosphatidylserine-binding protein that can be used for the detection of apoptosis. However, necrotic cells can also be labeled by Annexin V. Since loss of membrane integrity is a feature of necrotic cells, we utilize 7AAD, a membrane-impermeant dye to distinguish cells under early apoptosis

(AnnexinV+/7AAD- cells) and late apoptosis or necrosis (AnnexinV+/7AAD+). Our results have shown that there is a clear migration of cells under early apoptotic process at 5.0µg/mL of FKB to a late state of death at the concentrations of FKB 10 and 20µg/mL. Although our findings suggest that OVCAR-3 cells are dying through apoptosis, we cannot discard the possibility that, especially in higher concentrations of FKB, cells dye through necrotic mechanisms as well.

It has been shown that FKB is less cytocidal towards normal cells than to cancer cells (ABU *et al*, 2013). In the present work we have shown that FKB has a more pronounced action against OVCAR-3 cells than to primary human fibroblasts cells, especially at the concentration of 12.5µg/mL where there is a pronounced reduction of 80% on OVCAR-3 cells viability compared to a slightly decrease of 20% on fibroblasts viability. FKB reached a similar IC_{50} against the human fibroblasts established in our laboratory compared to other normal cells tested and described in the literature (Zi & Simoneau, 2005; Li *et al*., 2008; Kuo *et al.*, 2010; Tang *et al.*, 2010; Zhou *et al.*, 2010; An *et al.*, 2012; Eskander *et al.*, 2012; Hseu *et al.*, 2012; Li *et al.,* 2012; Lin *et al.*, 2012; Sakai *et al.*, 2012; Ji *et al.*, 2013; Kwon *et al.*, 2013; Abu *et al.*,2014, Abu *et al*., 2015).

The therapeutic index (TI) in drug development is considered the ratio of the highest exposure to the drug which results in no toxicity to the exposure that produced the desired efficacy. A high TI is preferable for a drug in terms of safety of use, whereas lower TI may be acceptable for the treatment of life-threatening diseases with limited therapeutic options (Muller & Milton, 2012). *In vitro* studies are the start point for drug development and consider the IC_{50} of target and non-target cells to determine selectivity. The selectivity index

calculated as the ratio between the IC_{50} of FKB towards fibroblasts and OVCAR-3 in the present work has indicated that FKB was two times more specific towards ovarian cancer cells than to normal cells. Although the narrow safety margin of FKB encountered in our *in vitro* study, some *in vivo* experiments showed no toxicity in mouse exposed to subcutaneously injection or oral intake high doses of FKB (Li *et al.,* 2012; Lin *et al.*, 2012; A*bu et al.,* 2015). Moreover, cisplatin, one of the most conventional and effective chemotherapeutics in the treatment of ovarian cancer, revealed an *in vitro* IC_{50} ranging from 25.7 to 100µM against OVCAR-3 cells in the literature, which is higher than the IC_{50} of FKB towards the same cells in our study (Smith *et al*.,2005; Wang *et al*., 2015). However, for a better toxicity comparison cisplatin should be also used to treat our fibroblasts cells. Therefore, more *in vitro and vivo* experiments, especially with orthotropic tumor models should be done to better access the pharmacodynamics and therapeutic index of FKB.

Many reports have described that FKB apoptotic effect especially involves the mitochondrial pathway with cleavage of caspase 9/3, downregulation of anti-apoptotic proteins and upregulation of pro-apoptotic proteins (Tang *et al.*, 2010; An *et al.*, 2012; Hseu *et al.,* 2012; Li *et al.*, 2012; Lin *et al.*, 2012; Abu *et al.*, 2013; Ji *et al.*, 2013). It was also described that the extrinsic pathway might be involved via upregulation of death receptor 5 (DR5) (Tang *et al.*, 2010).

The intrinsic apoptotic pathway is triggered by a change in the inner mitochondrial membrane permeability and potential, resulting in the release of sequestered pro-apoptotic proteins into the cytosol, such as cytochrome c and AIF. Cytochrome c binds to Apaf-1 and pro-caspase-9, forming the apoptosome. Activated caspase-9 further activates downstream

pro-caspase-3, which is the main apoptotic protease effector. On the other hand, AIF direct translocates to the nucleus, causing DNA fragmentation through a caspase independent mechanism (Fulda & Debatin, 2006; Elmore, 2007). The regulation of this mitochondrial permeability and death pathway occur thought members of Bcl-2 family proteins, which can be either pro-apoptotic, such as Bcl-2 and Bcl-xL or anti-apoptotic, including Bak, Bax, Bid, Bad, Bim and Bik (Elmore, 2007).

The Bcl-2 family proteins play important role in cancer by promoting tumor development and survival. EOC tumors overexpressing Bcl-2, the major inhibitor of apoptosis, are often found to be resistant to chemotherapy (Mano *et al.*, 1999). Recently, Wang *et al.* (2015) have shown that endogenous Bcl-2 levels of ovarian cancer cells, was positively correlated with sensitivity to cisplatin *in vitro*. OVCAR-3 was one of the cell lines utilized in the study and have demonstrated to possess high expression of Bcl-2 mRNA, being more resistant to cisplatin treatment than other cells with lower Bcl-2 mRNA levels. Our data demonstrated that FKB treatment of OVCAR-3 cells caused dowregulation of Bcl-2 anti-apoptotic protein, but did not change Bcl-xL expression. These results are in accordance with other publications that have shown reduction on Bcl-2 protein levels upon treatment with FKB in several cancer cell lines (Hseu *et al.*, 2012; Lin *et al.*, 2012; Sakai *et al.*, 2012; Ji *et al.*, 2013). Therefore, we suggest that FKB could be an important adjuvant drug to overcome chemotherapy resistance in epithelial ovarian cancer by the facilitation of apoptosis.

Bax and Bak proteins functions as apoptotic activators by inducing mitochondrial membrane permeabilization and release of cytochrome c. Bak is inserted in the mitochondrial wall, whereas Bax is predominantly cytosolic and translocated to the

mitochondrial outer membrane when activated (Westphal *et al.*, 2011). Bax gene encodes different splicing proteins, including Baxα (21kDa) and Baxβ (24kDa), both involved in apoptosis (Fu *et al.*, 2008). It has been extensively described a Bax overexpression in cancer cells exposed to FKB (Tang *et al*., 2010; An *et al*., 2012; Lin *et al*., 2012; Hseu *et al*., 2012; Sakai *et al.*, 2012; Ji *et al.*, 2013, Tang *et al.*, 2015). Our results have shown that the expression of the apoptotic proteins Bak and Bax did not significantly change upon treatment with FKB, although there was a tendency of increase in Bax protein expression. Considering that Bax protein heterodimerizes with Bcl-2 and inhibitis its activity, the Bax:Bcl-2 ratio indicates an activated mitochondrial death pathway and suscepti bility to apoptosis (Basu & Haldar, 1998, Das *et al*.,2004). According to our findings, there is a significant increase in the Bax:Bcl-2 ratio in OVCAR-3 at the concentration of 10µg/mL of FKB, indicating an activated mitochondrial death pathway.

Bcl-2 also controls the release of AIF protein, involved in the initiation of a caspase-independent pathway of apoptosis. Our results reveal that there was a tendency of AIF up regulation on OVCAR-3 cells treated with FKB, but not statically significant probably because of the high variability between experiments. Therefore, more experiments should be done in order to increase sample size and better determine AIF involvement in FKB mediated cell death.

The PI3K/Akt signaling cascade represents one of the most frequently deregulated pathways in cancer, by promoting cell proliferation, tumorigenesis and metastasis (Engelman, 2009). Akt is also the major mediator of survival signals that contributes for cancer cells evasion from apoptosis. It is commonly upregulated in epithelial ovarian cancer

and has been related to poor prognosis and chemoresistant diseases to paclitaxel and cisplatin (Al Sawah *et al.*, 2013; Bai *et al.*, 2016). The Cancer Genome Atlas Research Network (2011), has identified activation of the PI3K/AKT pathway in 40 percent of high-grade serous ovarian cancers through somatic copy number alterations. Therefore, pharmacological agents that inhibit Akt activation are a current research target for the discovery of new therapeutic strategies against ovarian cancer (Al Sawah *et al.*, 2013). One of the drugs under study is Perifosine, a synthetic alkylphospholipid and Akt inhibitor that has shown promising antiproliferative effects against ovarian cancer cells, also potentiating the anti-neoplasic effects of cisplatin (Sawah *et al.*, 2013). According to other publications, the kava-kava compounds, FKB and FKC, have also shown to dramatically inhibit Akt/PI3K pathway in human oral carcinoma and colon cancer cell lines respectively (Hseu *et al.*,2012; Phang *et al*.,2016).

Considering the clinical relevance for Akt inhibition on EOC, we investigated whether FKB could also affect PI3K/Akt cascade on OVCAR-3 cells by assessing Akt phophorylation. Akt is a serine-threonine kinase, which is activated by the phosphorylation of its both residues. In the present work, Western Blot analysis has shown that there was a significant inhibition of Akt activation identified by a decrease on its threonine residue phosphorylation in a dose-dependent manner. The total Akt expression, however, remained the same after treatment. Our results are very interesting, since there was a potent inhibition of Akt activation even at very low concentrations of FKB (2.5μg/mL) that didn't cause any toxic effects against normal cells. Our data reaffirms FKB as a promising strategy to overcome chemotherapy resistance in the management of ovarian cancers, especially on those presenting Akt amplification and *PTEN* gene loss.

Angiogenesis is a complex multistep process, involving cell proliferation, migration and tube formation. It is a critical step for tumor growth and metastasis. When a tumor lesion grows beyond 1-2mm, hypoxia triggers neovascularization signals to allow cancer progress (Weis & Cheresh, 2011). Numerous growth factors and cytokines are involved in this process, but VEGF is its major key mediator (Hanahan & Weinberg *et al.*, 2011).

The identification of antiangiogenic drugs is a new target for antineoplastic therapy, as shown by the positive results in the treatment of cancer patients with Bevacizumab, a monoclonal anti-VEGF antibody (Gadducci *et al*., 2015). The use of antiangiogenic therapy is also one of the most promising strategies in the treatment of ovarian cancer, revealing clinical efficacy both as single agents as well as in combination with chemotherapy (Coward *et al*., 2015). However the benefits of these drugs also come with toxic effects, such as bleeding, thromboembolism events, high blood pressure and perforation (Coward *et al*., 2015).

Previous reports have suggested that FKB could have an anti-metastatic action. Lin *et al.* (2012) have identified that FKB treatment reduced the expression of metastasis-related proteins, such as matrix metalloproteinase-9 (MMP-9) and urokinase plasminogen activator (u-PA) on human squamous carcinoma cells. Moreover, Abu *et al*. (2015) have found evidences using the clonogenic assay and bone marrow smearing assay that FKB reduced metastatic process in a breast cancer mice xenograft model. In addition, these authors on the basis of the proteome profile of tumors, have noticed that FKB reduced the expression of many pro-angiogenic related proteins, including angiogenin, coagulation factor 3, SDF-1, serpin F1, TSP-2, pentraxin 3 and VEGF. In addition, very recently, Abu *et al*. (2016)

demonstrated that FKB inhibited cell migration and tube formation *in vitro*, reduced sprouting vessels from an ex-vivo rat aortic ring assay and regulated many tyrosine kinase angiogenesis related proteins in breast cancer cells, such as VEGF. However, the FKB anti-angiogenic action utilizing an *in vivo* model has not been demonstrated yet.

Altogether, considering the clinical relevance of the anti-angiogenic therapy against EOC and the previous reports about FKB anti-metastatic action, the present work has confirmed the antiangiogenic effects of FKB *in vitro* and demonstrated, for the first time, the antiangiogenic potential of FKB *in vivo*.

Within the process of angiogenesis, recruited endothelial cells undergo migration, proliferation and differentiation. There are a number of *in vitro* experiments to evaluate angiogenesis and HUVEC cells are commonly used, for it is easily isolated from the umbilical vein (Staton *et al*., 2009; Abu *et al*., 2016). However, HUVECs are part of the macrovasculature while angiogenesis more often involves the microvasculature. For this, when studying angiogenesis it is important to access different types of endothelial cell lines (Staton *et al*., 2009). In our study we have used HUVEC and HBMEC cells, representative of the macrovasculature and microvasculature respectively.

Endothelial cells need to proliferate within the process of angiogenesis, thus we evaluated the FKB action towards HUVEC and HBMEC cell growth by the MTT assay. FKB didn't change HBMEC cells viability on the concentrations tested. On the other hand, HUVEC cells showed a significant reduction on cell viability at the concentrations of 5.0; 7.5 and 10µg/mL.

Moreover, angiogenesis requires endothelial cells to degrade the basement membrane in order to migrate into the perivascular stroma. Hence, to investigate cell migration ability, the wound healing assay was performed. It is based on the premise that endothelial cells in monolayer need to migrate for covering the denude area after scratching (Liang *et al*., 2007). Our results showed that FKB treatment significantly inhibited HUVECs cells migration at low concentrations (2.5µg/mL), which didn´t change HUVEC cell viability according to the MTT assay. Abu *et al.* (2015) also have performed wound healing assay, but with human breast cancer cells and described a reduction of about 50% on wound closure after treatment with FKB 9 µg/mL. The wound healing assay has the advantage of being easily performed but have been criticized because it might also involve multiple process rather than just cell migration, such as spreading and proliferation. Moreover, it is difficult to ensure that control and experimental groups are run into identical conditions of confluence and that the initial denude area is the same for all groups, limiting analysis (Staton *et al*., 2009).

The tube formation assay represents later steps on the angiogenic process that involve differentiation. It is based on the premise that endothelial cells plated onto a layer of gel matrix (Matrigel) are stimulated to attach, migrate and differentiate into tubule like structures, simulating the *in vivo* process (Arnaoutova & Keinman, 2010). The variables used to determine tubule formation are the average of tube length, number of tubules, tubule area and number of branch points. We have performed tube formation assay with HBMEC and HUVEC cells and the observation of tubule structures was performed respectively, through time lapse microscopy and with a stereomicroscope linked with a digital camera to photograph different fields.

Both experiments have demonstrated a clear reduction on tube formation upon FKB treatment of endothelial cells. Time lapse microscopy performed with HBMEC cells, revealed that FKB impairs tube formation even in the presence of VEGF, a potent pro-angiogenic factor. Going further, the tube formation assay with HUVECs allowed the quantification of tube formation by the number of tubule structures and branch points. It has demonstrated a significant dose-dependent reduction on endothelial cell differentiation into capillary structures under FKB treatment. At the concentration of 2.5µg/mL, which didn't show any toxicity towards endothelial cells, we can see a decrease of around 62% on branch points and 75% on total tubules formation. FKA, another chalcone of kava-kava extract, have also shown to cause inhibition of tube formation of HUVEC cells (ABU *et al*, 2014). Recently, similar to our results, Abu *et al*. (2016) have demonstrated that FKB inhibited HUVEC tube formation in a dose-dependent manner.

Zebrafish (*Danio rerio*) is a small tropical freshwater fish that yields hundreds of embryos per mating. It possesses a complex circulatory system, sharing genes and mechanisms of angiogenesis with mammals and provides many advantages compared to other vertebrate angiogenesis model systems (Nicoli & Presta, 2007).

In zebra fish circulatory system, the dorsal aorta and posterior cardinal vein are formed by vasculogenesis, while the SIVs and intersegmental vessels by angiogenesis, which can be easily, monitored in the study of new antiangiogenic drugs (Staton *et al*, 2009). Alkaline phosphatase (AP) staining is one of the methods to visualize vasculature, as endothelial cells express relatively high levels of endogenous AP activity (Serbedzija *et al*.,

1999). In order to confirm our *in vitro* findings regarding to the FKB antiangiogenic action, we utilized the zebrafish AP staining angiogenesis model.

Zebra fish exposure to increasing concentrations of FKB has demonstrated an impressive dose-dependent reduction on SIVs and intersegmental vessels formation, as well as a disruption of the vascular morphology of SIVs. The concentration of 2.5µg/mL FKB produced maximal desired effect (complete inhibition of SIV formation) with no toxicity against zebra fish larvae, being considered the ideal concentration according to our results. The measure of larvae length 48 hpf and 72 hpf also have proved that the embryos are growing and developing in the presence of FKB, so vascular impairment might not be due to postponed maturation. For the best of our knowledge, this was the first study that has demonstrated *in vivo* the antiangiogenic action of FKB. Taken all together, these remarkable results identify FKB as a potential anti-metastatic drug even at very low concentrations.

6 CONCLUSIONS

Ovarian cancer is a life threatening disease with high mortality and recurrence rates after aggressive treatment. Much effort has been done in order to discover new chemotherapy drugs to improve survival.

The present work has showed that FKB was able to reduce ovarian cancer cell viability in a time and dose-dependent manner, with less cytotoxic effects against normal cells. We have demonstrated that apoptosis might be the mainly mechanism of cell death, by the evaluation of cell morphology and flow cytometry analyzes.

The investigation of apoptotic and anti-apoptotic proteins expression has identified Bcl-2 downregulation and increased Bax:Bcl-2 ratio upon treatment with FKB. In addition, FKB has dramatically reduced Akt activation, even at very low concentrations.

The anti-angiogenic potential of FKB demonstrated in other studies was confirmed by our data and we have demonstrated for the first time that FKB also impairs angiogenesis *in vivo* in a zebrafish model.

Altogether, this study identifies, Flavokawain B as a novel promising additional drug in the treatment of ovarian cancer, by cell death induction, downregulation of cell survival pathways and inhibition of angiogenesis. However, it is just the beginning of a long journey in order to better comprehend the mechanisms of action and anti-cancer potential of FKB. Therefore, more studies are necessary aiming to determine FKB toxicity, therapeutic index and metabolism *in vivo*. Experiments accessing FKB action in combination with cisplatin should also be done to investigate its adjuvant effects at lower concentrations. Moreover,

the molecular mechanism involved in FKB antiangiogenic activity should be better elucidated.

7 REFERENCES

Abu N, Akhtar MN, Yeap SK, Lim KL. Ho WY, Zulfadli AJ, Omar AR, Sulaiman MR, Abdullah MP, Alitheen NB. Flavokawain A induces apoptosis in MCF-7 and MDA-MB231 and inhibits the metastatic process *in vitro*. *PloS One* 2014;9: 1-12.

Abu N, Ho WY, Yeap SK, Akhtar MN, Abdullah MP, Omar AR, Alitheen NB. The flavokawains: uprising medicinal chalcones. *Cancer Cell International* 2013;13:1-7.

Abu N, Mohamed NE, Yeap SK, Lim KL, Akhtar MN, Zulfadli AJ, Kee BB, Abdullah MP, Omar AR, Alitheen NB. *In vivo* antitumor and antimetastatic effects of flavokawain B in 4T1 breast cancer cell-challenged mice. *Drug design, development and therapy* 2015;9:1401-1417.

Abu N, Akhtar MN, Yeap SK, Lim KL, Ho WY, Abdullah MP, Ho CL, Omar AR, Ismail J, Alitheen NB. Flavokawain B induced cytotoxicity in two breast cancer cell lines, MCF-7 and MDA-MB231 and inhibited the metastatic potential of MDA-MB231 via the regulation of several tyrosine kinases *In vitro. BMC Complementary Alternative Medicine* 2016; 16: 1-14.

Al Sawah E, Chen X, Marchion DC, Xiong Y, Ramirez IJ, Abbasi F, *et al*. Perifosine, an AKT inhibitor, modulates ovarian cancer cell line sensitivity to cisplatin-induced growth arrest. *Gynecology Oncology* 2013;131:207–212.

An J, Gao Y, Wang J, Zhu Q, Ma Y, Wu J, Sun J, Tang Y. Flavokawain B induces apoptosis of non-small cell lung cancer H460 cells via Bax-initiated mitochondrial and JNK pathway. *Biotechnology Letters* 2012;34:1789-1790.

Armstrong DK, Bundy B, Wenzel L, Huang HQ, Baergen R, Lele S, Copeland LJ, Walker JL, Burger RA, Gynecologic Oncology Group. Intraperitoneal cisplatin and placitaxel in ovarian cancer. *The New England Journal of Medicine* 2006;354:34-43.

Arnaoutova I., Kleinman H. K. *In vitro* angiogenesis: endothelial cell tube formation on gelled basement membrane extract. *Nature Protocols* 2010; 5: 628–635.

Bai H, Cao D, Yang J, Li M, Zhang Z, Shen K. Genetic and epigenetic heterogeneity of epithelial ovarian cancer and the clinical implications for molecular targeted therapy. *Journal of Cellular and Molecular Medicine* 2016;20:1-13.

Basu A, Haldar S. The relationship between Bcl2 and p53: consequences for cell cycle progression and cell death. *Molecular Human Reproduction* 1998; 4: 1099-1109.

Borley J, Brown R. Epigenetic mechanisms and therapeutic targets of chemotherapy resistance in epithelial ovarian cancer. *Annals of Medicine* 2015;47:359-369

Bradford, M. M. A rapid and sensitive method for the quantitation of microgram quantities of protein utilizing the principle of protein-dye binding. *Analytical biochemistry* 1976; 72: 248-254.

Cancer Genome Atlas Research Network. Integrated genomic analyses of ovarian carcinoma. *Nature* 2011;474:609–615.

Cheaib B, Auguste A, Leary A. The PI3K/Akt/mTOR pathway in ovarian cancer: therapeutic opportunities and challenges. *Chinese Journal of cancer*. 2015; 34:4-16.

Chen L-M, Berek JS. Epithelial carcinoma of the ovary, fallopian tube and peritoneum: Epidemiology and risk factors. In: UpToDate, Post TW(Ed), UpToDate, Waltham, MA. (Accessed on March 26, 2016).

Chien JR, Aletti G, Bell DA, Keeney GL, Shridhar V, Hartmann LC. Molecular Pathogenesis and Therapeutic Targets in Epithelial Ovarian Cancer. *Journal of Cellular Biochemistry*. 2007;102:1117-1129.

Cho SG, Yi Z, Pang X, Yi T, Wang Y, Luo J, Wu Z, Li D, Liu M. Kisspeptin-10, a KISS1-derived decapeptide, inhibits tumor angiogenesis by suppressing Sp1-mediated VEGF expression and FAK/Rho GTPase activation. *Cancer Research* 2009;69:7062-7070.

Colombo N, Conte PF, Signata S, Raspagliesi F, Scambia G. Bevacizumab in ovarian cancer: Focus on clinical data and future perspectives. *Critical Reviews in Oncology/Hematology* 2016;97:335-348.

Coward JI; Middleton K.; Murphy F. New perspectives on target therapy in ovarian cancer. *International Journal of women's Health* 2015;7:189-203.

Das A, Banik NL, Patel SJ, Ray SK. Dexamethasone protected human glioblastoma U87MG cells from temozolomide induced apoptosis by maintaining Bax:Bcl-2 ratio and preventing proteolytic activities. *Molecular Cancer* 2004;3:1-10.

De Picciotto N, Cacheux W, Roth A, Chappuis PO, Labidi-Galy SI. Ovarian cancer: Status of homologous recombination pathway as a predictor of drug response. *Critical reviews in Oncology/Hematology* 2016.doi: 10.1016/j.critrevonc.2016.02.014.

Della Pepa C, Tonini G, Pisano C, DiNapoli M, Cecere SC, Tambaro R, Facchini G, Pignata S. Ovarian cancer standard of care: are there real alternatives? *Chinese journal of cancer* 2015;31:17-27.

Denizot F. & Lang R. Rapid colormetric assay for cell growth and survival. Modifications to the tetrazolium dye procedure giving improved sensitivity and reliability. *Journal of lmmunological Methods* 1986; 89: 271–277.

Dobbin ZC, Landen CN. The importance of the PI3K/AKT/MTOR pathway in the progression of ovarian câncer. *International Journal of Molecular Sciences* 2013;14:8213-8227.

Elmore S. Apoptosis: A Review of Programmed Cell Death. *Toxicology Pathology* 2007; 35:495-516

Engelman JA. Targeting PI3K signaling in cancer: opportunities, challenges and limitations. *Nature reviews* cancer 2009;9:550-562.

Eskander RN, Randall LM, Sakai T, Guo Y, Hoang B, Zi X. Flavokawain B, a novel naturally occuring chalcone, exhibits robust apoptotic effects and induces G2/M arrest of a uterine leiomyosarcoma cell line. *Journal of Obstetrics and Gynaecology Research* 2012;38:1086-1094.

Eskander RN, Tewari KS. Incorporation of anti-angiogenesis therapy in the management of advanced ovarian carcinoma – Mechanistics, review of phase III randomized clinical trials, and regulatory implications. *Gynecologic Oncology* 2014;132:496-505.

Feroz SR, Mohamad SB, Bujang N, Malek SNA, Tayyab S. Multispectroscopic and Molecular Modeling Approach To Investigate the Interaction of Flavokawain B with Human Serum Albumin. *Journal of Agricultural and Food Chemistry* 2012;60:5899-5908.

Friedman E, Kotsopoulos J, Lubinski J, T Lynch H, Ghadirian P, Neuhausen SL, Isaacs C, Weber B, Foulkes WD, Moller P, Rosen B, Kim-Sing C, Gershoni-Baruch R, Ainsworth P, Daly M, Tung N, Eisen A, I Olopade O, Karlan B, Saal HM, Garber JE, Rennert G, Gilchrist D, Eng C, Offit K, Osborne M, Sun P, Narod SA, and the Hereditary Breast Cancer Clinical Study Group. Spontaneous and therapeutic abortions and the risk of breast cancer among *BRCA* mutation carriers. *Breast Cancer Research* 2006;8: 1-7.

Fu NY, Sukumaran SK, Kerk SY, Yu VC. Baxβ: A Constitutively active human Bax isoform that is under tight regulatory controle by the proteosomal degradation mechanism. *Molecular Cell* 2009;33:15-29.

Fulda S, Debatin KM. Extrinsic versus intrinsic apoptosis pathways in anticancer chemotherapy. *Oncogene* 2006; 25:4798–4811.

Gadducci A, Lanfredini N, Sergiampietri C. Antiangiogenic agents in gynecological cancer: state of art and perspectives of clinical research. *Critical Reviews in Oncology/Hematology* 2015;96:113-128.

Hallare A., Nagel K., Kohler H. R. & Triebskorn R. Comparative embryotoxicity and proteotoxicity of three carrier solvents to zebrafish (Danio rerio) embryos. *Ecotoxicology and Environmental Safety* 2006; 63: 378–388.

Hamilton TC, Young RC, McKoy WM, Grotzinger KR, Green JA, Chu EW, Whang-Peng J, Rogan AM, Green WR, Ozols RF. Characterization of a human ovarian carcinoma cell line (NIH:OVCAR-3) with androgen and estrogen receptors. *Cancer Research* 1983; 43:5379-89.

Hanahan D, Weinberg RA. Hallmarks of cancer: the next generation. *Cell* 2011;144:646-674.

Hatzis C, Bedard PL, Birkbak NJ, Beck AH, Aerts HJ, Stem DF, Shi L, Clarke R, Quackenbush J, Haibe-Kains B. Enhancing reproducibility in cancer drug screening: how do we move forward? *Cancer Research* 2014;74:4016-4023.

Henderson BE, Kolonel LN, Dworsky R, Kerford D, Morri E, Singh K, Thevenot H. Cancer incidence in the islands of the Pacific. *National Cancer Institute Monograph* 1985;69:73-81

Hseu YC, Lee MS, Wu CR, Cho HJ, Lin KY, Lai GH, Wang SY, Kuo YH, Kumar KJ, Yang HL. The chalcone flavokawain B induces G2/M cell-cycle arrest and apoptosis in human oral carcinoma HSC-3 cells through the intracellular ROS generation and downregulation of the Akt/p38 MAPK signaling pathway. *Journal of Agricultural and Food Chemistry* 2012;60:2385-2397.

Instituto Nacional de Câncer José de Alencar Gomes da Silva. http://www2.inca.gov.br/wps/wcm/connect/tiposdecancer/site/home/ovario (Accessed on March 26, 2016).

Jaaback K, Johnson N. Intraperitoneal chemotherapy for the initial management of primary epithelial ovarian cancer (Protocol). *The Cochrane Database of Systematic Reviews* 2005;3:1-5.

Ji T, Lin C, Krill LS, Eskander R, Guo Y, Zi X, Hoang BH. Flavokawain B, a kava chalcone, inhibits growth of human osteosarcoma cells through G2/M cell cycle arrest and apoptosis. *Molecular Cancer* 2013;12:1-11.

Kim A, Ueda Y, Naka T, Enomoto T. Therapeutic strategies in epithelial ovarian cancer. *Journal of Experimental and Clinical Cancer Research* 2012;31:1-8.

Kimmel CB, Ballard WW, Kimmel SR, Ullmann B, Schilling TF. Stages of embryonic development of the zebrafish. *Developmental Dynamics*, 1995; 203:253-310

Kuo YF, Su YZ, Tseng YH, Wang SY, Wang HM, Chueh PJ. Flavokawain B, a novel chalcone from alpinia pricei hayata with potent apoptotic activity: involvement of ROS and GADD153 upstream of mitochondria-dependent apoptosis in HCT116 cells. *Free Radical Biology and Medicine* 2010;49:214-226.

Kurman RJ, Shih IeM. The dualistic model of ovarian carcinogenesis: revisited, revised and expanded. *The American Journal of Pathology* 2016;186:733-747.

Kurman RJ, Shih IeM. The origin and pathogenesis of epithelial ovarian cancer: a proposed unifying theory. *The American Journal of Surgical Pathology* 2010;34:433-443.

Kwon DJ, Ju SM, Youn GS, Choi SY, Park J. Supression of iNOS and COX-2 expression by flavokawain A via blockade of NF-kB and AP-1 activation in RAW 264.7 Macrophages. *Food and Chemical Toxicology* 2013;58:479-486

Leary A, Auclin E, Pautier P, Lhommé C. The PI3K/Akt/mTOR Pathway in Ovarian Cancer: Biological Rationale and Therapeutic Opportunities. In: Padilla-Díaz I. Ovarian Cancer – A Clinical and Translational uptodate. Croatia – European Union: Intech, 2013. P 275-302.

Leinster DA, Kulbe H, Everitt G, Thompson R, Perretti M, Gavins FN, Cooper D, Gould D, Ennis DP, Lockley M, McNeish IA, Nourshargh S, Balkwill FR. The peritoneal tumor microenvironment of high-grade serous ovarian cancer. *The Journal of Pathology* 2012;227:136-145.

Li N, Liu JH, Zhang J, Yu BY. Comparative evaluation of cytotoxicity and antioxidative activity of 20 flavonoids. *Journal of Agricultural and Food Chemistry* 2008;56:3876–83.

Li X, Liu Z, Xu X, Blair CA, Sun Z, Xie J, Lilly MB, Zi X. Kava components down-regulate expression of AR and AR splice variants and reduce growth in patient-derived prostate cancer xenografts in mice. *PLoS One* 2012;7:1-12.

Liang CC, Park AY, Guan JL. *In vitro* scratch assay: a convenient and inexpensive method for analysis of cell migration *in vitro*. *Nature Protocols* 2007;2:329–333.

Lin CT, Senthil Kumar KJ, Tseng YH, Wang ZJ, Pan MY, Xiao JH, Chien SC, Wang SY. Anti-inflammatory activity of flavokawain B from alpinia pricei hayata. *Journal of Agricultural and Food Chemistry* 2009, 57:6060-6065.

Lin E, Lin WH, Wang SY, Chen CS, Liao JW, Chang HW, Chen SC, Lin KY, Wang L, Yang HL. Hseu YC. Flavokawain B inhibits growth of human squamous carcinoma cells: involvement of apoptosis and cell cycle dysregulation *in vitro* and *in vivo*. *Journal of Nutricional Biochemistry* 2012;23:368-378.

Mahapatra DK, Bharti SK, Asati V. Anti-cancer chalcones: Structural and molecular target perspectives. *European Journal of Medicinal Chemistry* 2015; 98:69 -114.

Mano Y, Kikuchi Y, Yamamoto K, Kita T, Hirata J, Tode T, Ishii K, Nagata I. Bcl-2 as a predictor of chemosensitivity and prognosis in primary epithelial ovarian cancer. *European Journal of Cancer* 1999;35:1214–121.

Martin AC, Johnston E, Xing C, Hegeman AD. Measuring the chemical and cytotoxic variability of commercially available kava (Piper methysticum G.Forster). *PloS One* 2014;9:1-7.

Martins LCA. Regulação da expressão de genes relacionados à matriz extracelular em fibroblastos dérmicos de paciente com esquizofrenia. Tese (Doutorado em Medicina Molecular). Universidade Federal de Minas Gerais, Belo Horizonte, 2015.

Mohamad AS, Akhtar MN, Khalivulla SI, Perimal EK, Khalid MH, Ong HM, Zareen S, Akira A, Israf DA, Lajis N, Sulaiman MR. Possible participation of nitric oxide⁄cyclic guanosine monophosphate⁄protein kinase C⁄ATP-sensitive K + channels pathway in the systemic antinociception of flavokawin B. Basic and *Clinical Pharmacology and Toxicology* 2011;108:400-405.

Mohamad AS, Akhtar MN, Zakaria ZA, Perimal EK, Khalid S, Mohd PA, Khalid MH, Israf DA, Lajis NH, Sulaiman MR. Antinociceptive activity of a synthetic chalcone, flavokawain B on chemical and thermal models of nociception in mice. *European Journal of Pharmacology* 2010;647:103-109.

Muller & Milton. The determination and interpretation of therapeutic index in drug development. *Nature Reviews* 2012;11:751-761.

NCCN, 2016. NCCN clinical practice guidelines in oncology: Genetic/familial high-risk assessment-breast and ovarian. Version 1.20: Available from< www.nccn.org>.

Nicoli S, Presta M. The zebrafish/tumor xenograft angiogenesis assay. *Nature Protocols* 2007;2:2918-2923.

Nicoli S. & Presta M. The zebrafish/tumor xenograft angiogenesis assay. *Nature Protocols* 2007; 2: 2918–2923.

Parichy DM, Elizondo MR, Mills MG, Gordon TN, Engeszer RE. Normal table of postembryonic zebrafish development: staging by externally visible anatomy of the living fish. *Developmental Dynamics* 2009;12:2975-3015

Phang CW, Karsani SA, Sethi G, Abd Malek SN. Flavokawain C Inhibits Cell Cycle and Promotes Apoptosis, Associated with Endoplasmic Reticulum Stress and Regulation of MAPKs and Akt Signaling Pathways in HCT116 Human Colon Carcinoma Cells. *PLoS One* 2016;11:1-27.

Pinner KD, Wales CT, Gristock RA, Vo HT, So N, Jacobs AT. Flavokawains A and B from kava (Piper Methysticum) activate heat shock and antioxidant responses and protect against hydrogen peroxide-induced cell death in HepG2 hepatocytes. *Pharmacology Biology* 2016; 20:1-10.

Ramalingam P. Morphologic, Immunophenotypic, and Molecular Features of Epithelial Ovarian Cancer. *Oncology* 2016;30:166-176.

Sakai T, Eskander RN, Guo Y, Kim KJ, Mefford J, Hopkins J, Bhatia NN, Zi X, Hoang BH. Flavokawain B, a kava chalcone, induces apoptosis in synovial sarcoma cell lines. *Journal of Orthopaedic Research*2012;30:1045-1050.

Schayek H, De Marco L, Starinsky-Elbaz S, Rossette M, Laitman Y, Bastos-Rodrigues L, Silva Filho AL, Friedman E. The rate of recurrent BRCA1, BRCA2 and TP53 mutations in the general population, and unselected ovarian câncer cases, in Belo Horizonte, Brazil. *Cancer Genetics* 2016;209:50-52.

Scott CL, Swisher EM, Kaufmann SH. Poly (ADP-Ribose) Polymerase Inhibitors: Recent Advances and Future Development. *Journal of Clinical Oncology* 2015;33:1397-1406.

Serbedzija GN, Flynn E, Willet CE. Zebrafish angiogenesis: a new model for drug screening. *Angiogenesis* 1999;3:353-359.

Shaver JH, Sosis R. How does male ritual behavior vary across the lifespan? An examination of Fijian kava ceremonies. *Human nature* 2014;25:136-160.

Showman AF, Baker JD, Linares C, Naeole CK, Borris R, Johnston E, Konanui J, Turner H. Contemporary Pacific and Western perspectives on `awa (Piper methysticum) toxicology. *Fitoterapia* 2015;100:56-67.

Siegel R, Ma J, Zou Z, Jemal A. Cancer statistics 2014. CA *Cancer Journal of Clinicians* 2014; 64:9-29.

Singh YN, Devkota AK. Aqueous kava extracts do not affect liver function tests in rats. *Planta Medica* 2003; 69:496-499.

Singh YN. Kava: an overview. *Journal of Ethnopharmacol* 1992;37:13–45.

Smith JA, Ngo H, Martin MC, Wolf JK. An evaluation of cytotoxicity of the taxane and platinum agents combination treatment in a panel of human ovarian carcinoma cell lines. *Gynecology Oncology.* 2005;98:141-145.

Sociali G, Raffaghello L, Magnone M, Zamporlini F, Emionite L, Sturla L, Bianchi G, Vigliarolo T, Nahimana A, Nencioni A, Raffaelli N, Bruzzone S. Antitumor effect of combined NAMPT and CD73 inhibition in an ovarian cancer model. *Oncotarget.* 2016 ;7:2968-84.

Sorensen RD, Schnack TH, Karlsen MA, Hogdall CK. Serous ovarian, fallopian tube and primary peritoneal cancers: a common disease or separate entities – a systematic review. *Gynecologic Oncology* 2015;136:571-581.

Staton C. A., Reed M. W., Brown N. J. A critical analysis of current *in vitro* and *in vivo*angiogenesis assays. International. *Journal of Experimental Pathology*, 2009; 90: 195–221.

Steiner GG. The correlation between cancer incidence and kava consumption. *Hawaii Medical Journal*. 2000;59:420–422.

Tang Y, Li X, Liu Z, Simoneau AR, Xie J, Zi X. Flavokawain B, a kava chalcone, induces apoptosis via up-regulation of death-receptor 5 and Bim expression in androgen receptor negative, hormonal refractory prostate cancer cell lines and reduces tumor growth. *Internacional Journal of Cancer*. 2010;127:1758-1768.

Tang YL, Huang LB, Tian Y, Wang LN, Zhang XL, Ke ZY, Deng WG, Luo XQ. Flavokawain B inhibits the growth of acute lymphoblastic leukemia cells via p53 and caspase-dependent mechanisms. *Leukemia Lymphoma.* 2015;56:2398-23407.

Teschke R, Qiu SX, Lebot V. Herbal hepatotoxicity by kava: update on pipermethystine, flavokavain B, and mould hepatotoxins as primarily assumed culprits. *Digestive and Liver Disease.* 2011;43:676-681

Vincent EE, Elder DJ, Thomas EC, Phillips L, Morgan C, Pawade J, Sohail M, May MT, Hetzel MR, Tavaré JM. Akt phosphorylation on Thr308 but not on Ser473 correlates with Akt protein kinase activity in human non-small cell lung cancer. *British Journal of Cancer*. 2011;104:1755-1761.

Vistica DT, Skehan P, Scudiero D, Monks A, Pittman A, Boyd MR. Tetrazolium-based assays for cellular viability: a critical examination of selected parameters affecting formazan production. *Cancer Research* 1991; 15:2515-2520.

Wang H, Zhang Z, Wei X, Dai R. Small molecule inhibitor of Bcl-2 (TX-37) suppresses growth and enhances cisplatin-induced apoptosis in ovarian cancer cells. *Journal of Ovarian Research.* 2015;20:2-8.

Wang Z, Fu S. An overview of tyrosine kinase inhibitors for the treatment of epithelial ovarian cancer. *Expert Opinion on Investigational Drugs*. 2015; 25:15-30.

Weis SM, Cheresh DA. Tumor angiogenesis: molecular pathways and therapeutic targets. *Nature Medicine* 2011;17: 1359–1370

Westphal D, Dewson G, Czabotar PE, Kluck RM. Molecular biology of Bax and Bak activation and action. Biochimica et Biophysica Acta (BBA) - *Molecular Cell Research* 2011; 1813: 521–531.

Wollenweber E, Rehse C, Dietz VH. The occurence of aurentiacin and flavokawain B on pityrogramma triangularis Var. Pallida and didymocarpus species. *Phytochemistry* 1981;20:1167-1168.

Wu D, Nair MG, Dewitt DL. Novel compounds from piper methysticum forst (kava kava) roots and their effect on cyclooxygenase enzyme. *Journal of Agricultural and Food Chemistry* 2002;50:701-705.

Zhou P, Gross S, Liu JH, Yu BY, Feng LL, Nolta J, Sharma V, Piwnica-Worms D, Qiu SX. Flavokawain B, the hepatotoxic constituent from kava root, induces GSH-sensitive oxidative stress through modulation of IKK/NF-κB and MAPK signaling pathways. *The Federation of American Societies for Experimental Biology Journal* 2010;24:4722-4732.

Zi X, Simoneau AR. Flavokawain A, a novel chalcone from kava extract, induces apoptosis in bladder cancer cells by involvement of Bax protein-dependent and mitochondria-dependent apoptotic pathway and suppresses tumor growth in mice. *Cancer Research* 2005;65:3479–3486.